MSc Program Building Science & Technology

Derivation of diffuse irradiance based on measured global irradiance data

A master's thesis submitted for the degree of
"Master of Science"

Supervisor: Univ. Prof. Dipl. Ing. Dr. Techn. A. Mahdavi
Department of Building Physics and Building Ecology

Ing. Katerina Zavodnikova
Vienna, 25.09.2010
0827194

Affidavit

I, Katerina Zavodnikova hereby declare

1. That I am the sole author of the present Master Thesis, " Derivation of diffuse irradiance based on measured global irradiance data ", 100 pages, bound, and that I have not used any source or tool other than those referenced or any other illicit aid or tool, and

2. That I have not prior to this date submitted this Master Thesis as an examination paper in any form in Austria or abroad.

Prague, Date Signature

_____ _____

ACKNOWLEDGEMENT

I would like to use this possibility to thank my supervisor Prof. Dr. Ardesir Mahdavi, the Head of the Department of Building Physics and Building Ecology, for guiding me towards the formulation and realization of this in-depth research project.

I would like to thank Mr. J. Lechleitner for the data and pictures of meteo-station, MSc. S. Dervishi, PhD for the support and important advice and explanations of the thesis problems.

My friends Ing. Jan Bures and Ing Karel Vesely who supported the mathematical part of my thesis my gratitude belongs to them.

Finally, I would like to thank my parents and my brother for their support in making this effort worthwhile.

1. ABSTRACT

The topic of renewable energy use is important especially nowadays, when the main aim is to reduce the emission of carbon dioxide produced mainly by the use of fossil fuels. Renewable energy is considered a key source for the future and has many advantages compared to fossil fuels. Global irradiance is one of the important parameters that is necessary as an input for different solar systems. It is also an initial energy source for all ecosystems and because of this condition, it is necessary to have proper information and data about different kinds of radiation. There are still stations in many regions in every country that do not provide complete irradiation data, especially diffuse irradiation. This is the reason of estimating solar models with dependence of available data – global radiation. Estimation of solar radiation on a tilted surface is part of the design a solar power or solar thermal system.

This research offers the way to derive incident irradiance values on tilted building surfaces according to the solar model fitted to the weather data of Vienna. The calculation is based on the main input data – global irradiance values.

The eight known solar models are considered to compute the incident irradiance based on the measured global horizontal irradiance data. Values provided by calculations of solar models are compared with measurements in the station. Later on, the results are evaluated by the correlation of measured and calculated values of diffuse radiation. The correlation evaluation is based on relative error (RE), mean square deviation (MSD), and root means square deviation (RMSD).

The best behaved four models are used for creating of the proper solar models to Vienna´s climate condition. The Vienna models are applied for data measured in Czech Republic (Trebon). Based on Trebon´s data new solar models are created with modified coefficients that better fit the climate condition in the CR.

Keywords : solar irradiance, diffuse components, solar models, energy performance, tilted surfaces, measurement, weather data

TABLE OF CONTENTS

LIST OF FIGURES

LIST OF TABLES

2. INTRODUCTION

2.1. Summary

The surface of the Sun (the photosphere) has a granular structure and is permanently moving. The main amount of solar radiation is emitted from this surface layer. The transmittance from the photosphere to the Earth is not interrupted in its length of 150 mil. km and does not change in the time of its duration which is 8 minutes and 18 seconds.

The earth´s atmosphere does not transmit the long wave radiation evenly because it is influenced by the amount of clouds, air molecules, water vapour, dust, pollutants, forest fires and volcanoes.

In the middle of a cloudless day the irradiance is scattered and absorbed by about 25% of the solar irradiance, when it passes through the atmosphere. This irradiance, which incidents to the earth´s surface without being scattered is called direct normal irradiance (beam irradiance). Due to the direct radiation dispersing the diffuse radiation reaches the surface from every direction. The total solar radiation (the sum of the direct and diffuse radiation on the horizontal surface) is called global irradiance. According to the recent findings the global solar radiation and ambient air temperature changes have periodical character. [1]

From the total amount of radiation 70% falls from April to September and the last 30% falls between the October and March. During the clear skies the diffuse irradiation is 1/5 of the global irradiation, in the contrast, during a cloudy day the global irradiance is formed only by diffuse irradiation.

In middle Europe with dependence of season and the atmospheric condition the intensity of global irradiance at noon could vary between 100 and 1000 Wm^{-2}. The ration between direct and diffuse irradiance depends on geographic and microclimatic conditions. The diffuse irradiance counts as 50-70% of the amount of global irradiance per year in middle Europe and during the winter season reaches the 90%.

The incident solar radiation is influenced by the angle of the tilted surface. During summer months the highest amount of solar radiation reaches the surface with an optimal tilt of approximately 30°. The situation is different in winter, when the radiation more greatly incidents the surfaces at the higher angles of 64°-70°. The total irradiance is the sum of incident diffuse radiation and the direct normal irradiance projected onto the tilted surface as well as ground reflected irradiance that is incident on the tilted surface when the surface is tilted with respect to the horizontal.

2.2.Motivation

Solar heat gain and related solar irradiance are important components of evaluation of building environment and energy balance. Climatic data like air temperature, humidity and wind speed are usually more available than data of solar irradiance. The availability of this kind of data is limited, not every meteorological station provides measured diffuse irradiance. In the contrast the global irradiation is widely measured. Therefore it is quite essential to be able to calculate solar diffuse radiation incident on building surfaces also at different tilted angles. The correlation is the basic of diffuse component calculation of global horizontal radiation. The need of radiation data forced to develop some kind of radiation models that allow the calculation of radiation parameters with small deviation. Also the importance of this model rises with respect to the use of the solar energy. Diffuse radiation data are also useful for validating irradiative transfer models, and have applications in building design where day lighting is a consideration. Following lines describe cases, where diffuse radiation is important and the knowledge of exact value would help to the proper and effective design.

One way to renewable energy use is the design of photovoltaic panels, where the power depends on the intensity of the radiation. The intensity is also influenced by the sky condition (clear sky, cloudy). The technology of photovoltaic panels converts the energy from solar radiation to the electricity. The effect of photovoltaic is used in photovoltaic systems. The primary input of the energy for PV is the solar radiation, intensity of radiation, composition and the total duration. This parameters influence the efficiency of photovoltaic panels and the amount of power produced. It is known, that mono and multi-crystalline solar cells need direct solar radiation to reach the maximum yield. On the other hand thin layer photovoltaic cells made based on amorphous silicon are able to use also the diffuse radiation. In the total amount of the annual energy those panels produce more energy compare to mono/multi-crystalline cells (approximately 10% higher production).

Solar thermal collectors are devices design to collect heat by absorbing sunlight and converting the energy of solar radiation into a more usable or storable form. Flat plate and evacuated tube solar collectors are used to collect heat for space heating or domestic hot water. Those devices allow the use of the solar energy

the whole year, also when is freezing or the cloudy day. The efficiency of solar systems is increased, when the solar radiation incidents the surface perpendicularly.

Shading devices such as venetian blinds, roller blinds, and drapes are effective method to the control of solar heat gain. Solar radiation increases cooling requirements of as much as 25% [3]. It is necessary to analyze the solar radiation on the whole external surfaces of the building to design the proper shading system. There is a strong need for models that allow shading layers to be included in glazing system analysis. The paper *Solar absorption by each element in a glazing/shading layer array* presents methods by which existing solar optical models for systems of specular glazing layers can be extended to include the effect of layers that create scattered, specifically diffuse, radiation in reflection and/or transmission. [4]

3. BACKGROUND

Several empirical models were developed by many researchers to predict the solar radiation for different location, among these models:

The possibility to estimate diffuse and direct irradiance is provided by two kind of different models:

a.) *Parametric models* (atmospheric transmittance models)

- Require information of atmospheric parameters (atmospheric turbidity, precipitable water, cloud cover

b.) *Decomposition models* (decomposition of global irradiance)

- Estimate direct and diffuse irradiance from global irradiance

- Based on correlation between *clearness index* k_t (glob. irrad./horizontal extraterrestrial irrad.) and the *diffuse fraction* k_d (diff.irrad./global. irrad)

Diffuse fraction depends also on variables: solar elevation, temperature and relative humidity

The main important equations for direct irradiance:

$$I_b = \frac{I_t \cdot (1 - k_d)}{sin\alpha}$$

$$k_d = \frac{I_d}{I_t};\ k_t = \frac{\frac{I_t}{I_o}}{sin\alpha};\ k_b = \frac{I_b}{I_o}$$

I_t is global radiation; I_b direct irradiance; α solar elevation angle; D diffuse radiation;

I_o extraterrestrial irradiance; k_t clearness index; k_d diffuse fraction; k_b direct transmittance

The present work involves decomposition models.

4. APPROACH

Based on past research of solar radiation, eight models were considered to derive the diffuse radiation from the measured global horizontal irradiance values. Those solar models are mainly suggested by L.T. Wong and W.K. Chow 2001 [1]. Each model will be described later on.

4.1. Model selection

The first step in this study is the comparison of diffuse radiation predicted by eight different models with measured values for Vienna (data obtained from the weather station of Vienna University of Technology). The results were evaluated by the correlation of measured and calculated values of diffuse radiation. The correlation evaluation is based on relative error (RE), mean square deviation (MBD) and root means square deviation (RMSD). Those statistic methods enable the detection of differences between measured data and model estimation. According to the evaluation were selected four solar radiation models: Erb´s, Reindl´s, Lam and Li´s, Orgill and Holland´s.

4.2. Modification of selected models

The four selected models were considered in two versions: the first was with original coefficients and the second with modified coefficient based on measured data in Vienna. The coefficients were changed according to the fitting curve and linear regression by the use of mathematic software. The main purpose of this step was to create the own solar model proper for Vienna. The behaviour of models according to the interval of k_d (describe sky condition – cloudy, partly cloudy, cloud less sky) was tested for each model.

4.3. Application of new models and comparison with different location

Modified solar models for Vienna were used together with original models to calculate diffuse radiation in Trebon. Those two models were compared also with the new model modified for Trebon data. The same process of evaluation was used in every cases.

5. MEASURING DEVICES

For the data collecting was used a sky monitoring device, designed at the Department of Building Physics and Building Ecology of Vienna University of Technology. This device is placed on the roof of a university building.

The data gathered from the sensors are stored by using the "Data-Log-Datasocket" software program and calibrated based on the measured global horizontal illuminance values.

The pyranometer could be sometimes called like solarimeter. This device is used to measure solar irradiance on a planar surface. This sensor is designed to measure the solar radiation flux density in W/m^2 from a field of view of 180 degree.

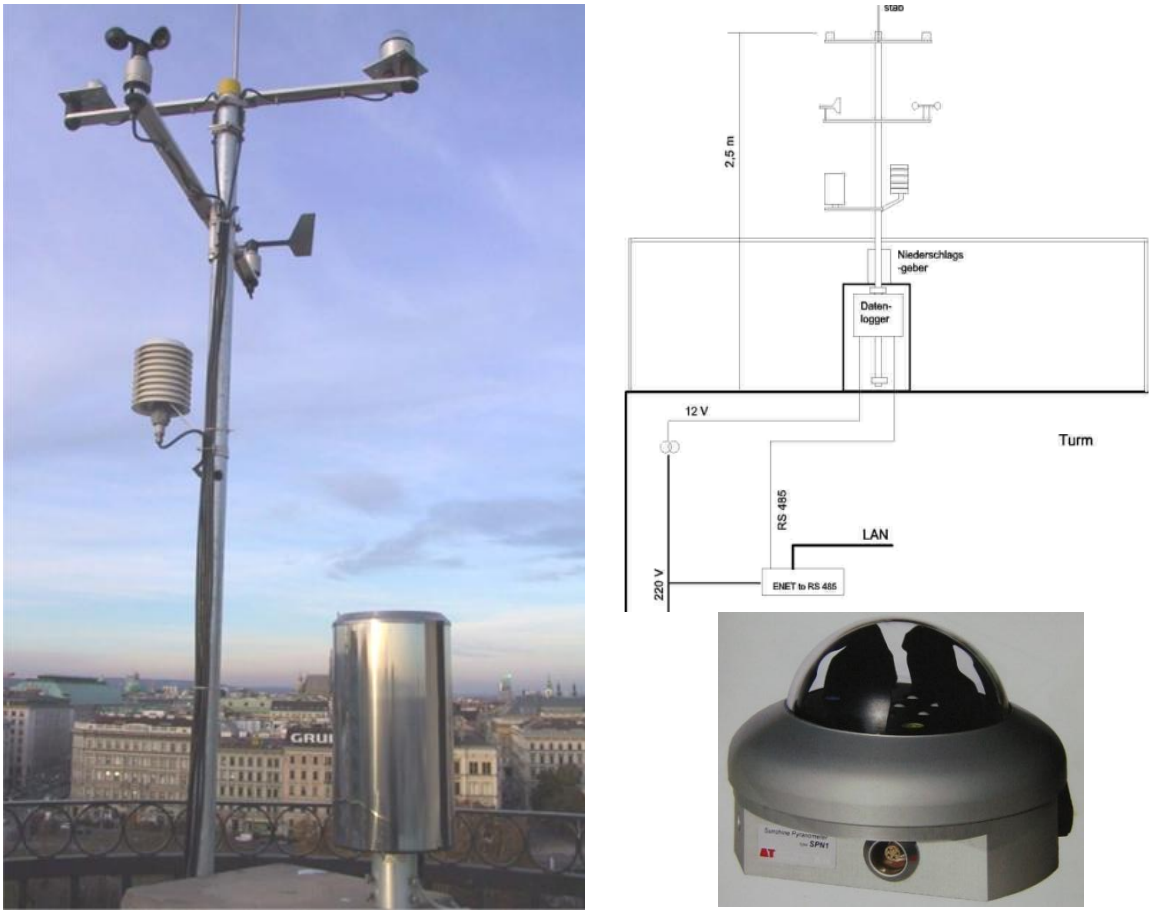

Figure 1 : Picture of the meto-station and sunshine pyranometer SPN1.

6. DERIVATION OF IRRADIANCE – SOLAR MODELS

There is used calculation of extraterrestrial radiation on horizontal surface (I_o) in every model, according to the following equation:

$$I_o = I_{sc} \cdot \left(1 + 0{,}33cos\frac{360n}{365}\right) \cdot cos\theta_z$$

where

I_{sc} solar constant, 1367 W m^{-2}; energy from the sun per unit time received on a unit surface area perpendicular to the direction of propagation of radiation at the earth mean distance from sun outside the atmosphere.

θ_z zenith angle of the sun (°)

n day of the year (-)

6.1. Erb´s model

Erb´s studied correlations between normal direct irradiance and global irradiance on a horizontal surface based on data measured in 5 stations in USA.

$$k_d = 1 - 0{,}09k_t \;\; ; \;\; k_t \leq 0{,}22$$

$$k_d = 0{,}9511 - 0{,}1604k_t \; + 4{,}388k_t^2 - 16{,}638k_t^3 + 12{,}336k_t^4; \;\; 0{,}22 < k_t \leq 0{,}8$$

$$k_d = 0{,}165 \qquad ; \;\; k_t > 0{,}8$$

where

$k_t = \frac{I_t}{I_o}$; $I_d = I_t \cdot k_d$

6.2. Reindl´s model

Reindl´s estimated diffuse fraction k_d based on measured data of global and diffuse irradiance on horizontal surfaces. He used the data base of global and diffuse irradiance from 5 locations in the USA and Europe (28-60°N latitude). The algorithm allows deriving the diffuse components from corresponding measured global horizontal irradiance values. The direct normal values are derived from the direct horizontal irradiance values.

The estimation of diffuse fraction k_d using clearness index k_t is given by those equations:

$$k_d = \frac{I_d}{I_t}$$

where

I_t hourly total radiation on a horizontal surface (W m^{-2})

I_d hourly diffuse radiation on a horizontal surface (W m^{-2})

1.)

Interval : $0 \leq k_t \leq 0,3$ Constraint : $I_d/I_t \leq 1,0$

$$k_d = 1,000 - 0,232k_t + 0,0239\sin\alpha - 0,000682T_a + 0,0195\Phi$$

Interval : $0,3 < k_t < 0,78$ Constraint : $0,1 \leq I_d/I_t \leq 0,97$

$$k_d = 1,329 - 1,716k_t + 0,267\sin\alpha - 0,00357T_a + 0,106\Phi$$

Interval : $k_t \geq 0,78$ Constraint : $I_d/I_t \geq 0,1$

$$k_d = 0,426k_t - 0,256\sin\alpha + 0,00349T_a + 0,0734\Phi$$

There were also developed models with less included multiple predictor variables [5]. The results comparison of this model variation difference is provided in this work.

2.)

Interval : $0 \leq k_t \leq 0,3$ Constraint : $I_d/I_t \leq 1,0$

$$k_d = 1,020 - 0,254k_t + 0,0123\sin\alpha$$

Interval : $0,3 < k_t < 0,78$ Constraint : $0,1 \leq I_d/I_t \leq 0,97$

$$k_d = 1,400 - 1,749k_t + 0,177\sin\alpha$$

Interval : $k_t \geq 0,78$ Constraint : $I_d/I_t \geq 0,1$

$$k_d = 0,486k_t + 0,182\sin\alpha$$

Derivation of diffuse irradiance based on measured global irradiance data

3.)

Interval : $0 \leq k_t \leq 0,3$ Constraint : $I_d/I_t \leq 1,0$

$$k_d = 1,020 - 0,248k_t$$

Interval : $0,3 < k_t < 0,78$ Constraint : $0,1 \leq I_d/I_t \leq 0,97$

$$k_d = 1,45 - 1,67k_t$$

Interval : $k_t \geq 0,78$ Constraint : $I_d/I_t \geq 0,1$

$$k_d = 1,47$$

k_t clearness index (-)
k_d diffuse fraction (-)
I_d total diffuse irradiance on a horizontal surface (W m^{-2})
I_t hourly total (global) radiation on a horizontal surface (MJ m^{-2})

The subsequent constraints are places on the correlation in each interval. They assure reasonable predicted values because is possible, that some combinations of predictors may produce unreasonable values of k_d.

6.3.Lam and Li´s

Lam and Li focused on the correlation between global solar radiation and its direct and diffuse components.

$$k_d = 0,977; \quad k_t \leq 0,15$$

$$k_d = 1,237 - 1,361k_t; \quad 0,15 < k_t \leq 0,7$$

$$k_d = 0,273 \quad ; \quad k_t > 0,7$$

where

k_t clearness index (-)
k_d diffuse fraction (-)

6.4. Orgill and Holand´s model

Orgill and Holland estimated diffuse fraction based on clearness index k_t (only variable). They used the data base of global and diffuse irradiance from Toronto (Canada) to create the model.

The correlation between the hourly diffuse fraction on a horizontal surface k_d and clearness index k_t is given by those equations:

$$k_d = 1 - 0{,}249k_t \;\; ; \;\; k_t < 0{,}35$$

$$k_d = 1{,}577 - 1{,}84k_t \;\; ; \;\; 0{,}35 \leq k_t \leq 0{,}75$$

$$k_d = 0{,}177 \;\; ; \;\; k_t > 0{,}75$$

where

$k_t = \frac{I_t}{I_o}$; $I_d = I_t \cdot k_d$

The direct irradiance I_b is obtained by :

$$\boldsymbol{I_b = \frac{I_t.(1 - k_d)}{sin \propto}}$$

k_t clearness index (-)
k_d diffuse fraction (-)
I_b total beam irradiance on a horizontal surface (W m^{-2})
I_t monthly average daily global radiation on a horizontal surface (W m^{-2})
α solar altitude (°)

6.5.Skartveit and Olseth´s model

Skartveit and Olseth estimated dependence of diffuse fraction k_d on other parameters (solar elevation, temperature and relative humidity. Similar arguments were taken to account by Reindl. The model was validated for more than 10 stations worldwide.

The estimation of direct irradiance I_b from global irradiance G_t is given by those equations:

$$\boldsymbol{I_b = \frac{G_t\,(1-\Psi)}{sin\,\propto}}$$

Interval : $k_t < c_1$

c_1=0,2

y= 1

Interval : $c_1 \leq k_t \leq 1{,}09\ c_2$

c_1=0,2

$y= 1-(1-d_1).\left[d_2 c_3^{1/2} + (1-d_2).c_3^2\right]$

where

$c_2 = 0{,}87 - 0{,}56e^{-0{,}06\propto}$

$c_3 = 0{,}5\left\{1 + sin\left[\pi\left(\frac{c_4}{d_3} - 0{,}5\right)\right]\right\}$

$c_4 = k_t - c_1$

$d_1 = 0{,}15 + 0{,}43e^{-0{,}06\propto}$

$d_2 = 0{,}27$

$d_3 = c_2 - c_1$

Interval : $k_t > 1{,}09\ c_2$

$y= 1 - 1{,}09c_2\frac{1-\xi}{k_t}$

where

$\xi = 1-(1-d_1)\left(d_2 c_3^{'}\frac{1}{2} + (1-d_2)c_3^{'2}\right)$

$c_3^{'} = 0{,}5\left\{1 + sin\left[\pi\left(\frac{c_4^{'}}{d_3} - 0{,}5\right)\right]\right\}$

$c_4^{'} = 1{,}09c_2 - c_1$

According to the conditions deviating from the validation domain constants have to be adjusted.

k_t clearness index (-)
I_b total beam irradiance on a horizontal surface (W m^{-2})
G_t monthly average daily global radiation on a horizontal surface (MJ m^{-2})
α solar altitude (degrees)
y function of k_t and the solar elevation
ξ tilt angle of a surface measured from the horizontal (degrees)
c_1, c_2, c_3, c_4, d_1, d_2, d_3, d_4, d_5, d_6 coefficients (-)

6.6.Maxwell´s model

Maxwell model estimated converting hourly global to direct normal insolation. This model is combination of physical model and experimental fits for other conditions.

The direct irradiance is given by this relation:

$$\boldsymbol{I_b = I_o\{\Psi - (d_4 + d_5 e^{m_a d_6})\}}$$

where

y= $0{,}866 - 0{,}122m_a + 0{,}0121m_a^2 - 0{,}000653m_a^3 + 0{,}000014m_a^4$

$m_a = m_r \frac{p}{1013{,}25}$;

$m_r = \frac{1}{cos\theta_z}$; Θ_z zenith angle

Interval : $k_t \leq 0{,}6$

$d_4 = 0{,}512 - 1{,}56k_t + 2{,}286k_t^2 - 2{,}222k_t^3$

$d_5 = 0{,}37 + 0{,}962k_t$

$d_6 = -0{,}28 + 0{,}923k_t - 2{,}048k_t^2$

Interval : $k_t > 0{,}6$

$d_4 = -5{,}743 + 21{,}77k_t - 27{,}49k_t^2 + 11{,}56k_t^3$

$d_5 = 41{,}4 - 118{,}5k_t + 66{,}05k_t^2 + 31{,}9k_t^3$

$d_6 = -47{,}01 + 184{,}2k_t - 222k_t^2 + 73{,}81k_t^3$

where

k_t clearness index (-)
I_b total beam irradiance on a horizontal surface (W m^{-2})
I_o hourly extraterrestrial radiation (MJ m^{-2})
y function of k_t and the solar elevation
d_4, d_5, d_6 coefficients (-)
m_a air mass at actual pressure (-)

6.7. Vignola and McDaniel´s model

The model was created based on the measurements in seven sites in Oregon and Idaho, USA (38-46°N latitude). This estimation takes in account the number of the day (N).

for $k_t \geq 0{,}175$

$$k_d = 0{,}013 - 0{,}175k_t + 0{,}52k_t^2 + 1{,}03 + (0{,}038k_t - 0{,}13k_t^2)sin[2\pi(N - 20)/365]$$

for $k_t < 0{,}175$

$$k_d = 0{,}125k_t^2$$

where

k_t clearness index (-)
N number of the day (-)

7. MEASUREMENTS

The data of input for solar models (Table 1) were obtained from the Department of Building Physics and Building Ecology of Vienna University of Technology. The data set was cleared from the irradiance during the night, when the solar altitude is lower than 5°. Data of global radiation measured by pyranometer with higher deviation than 5% were excluded from the database. The values of irradiance in the interval 50-1100 $W.m^{-2}$ were included to the database used for calculation of solar models.

The first database for the comparison of models in terms of accuracy contained measured values over a 2-years period (from July 2008 to March 2010), 30 263 pairs of measured irradiance. The second database used for validation and modification of selected solar models was used for the same season period (January 2007 to June 2008), 37 086 pairs was included.

Measurements of global and diffuse irradiance were performed every 5 minutes during all sky condition from sunny, partly cloudy to overcast.

The weather station also provided measurements of air temperature, air pressure and air relative humidity.

		Erbs	Reindl	Lam + Li	Orgill + Holland	Skartveit + Olseth	Maxwell	Louche	Vignola + McDaniels
I	global irradiance	×	×	×	×	×	×	×	×
N	nb. of the day	×	×	×	×	×	×	×	×
I	solar constant	×	×	×	×	×	×	×	×
α	solar altitude	×	×	×	×	×	×	×	×
Φ	relative humidity		×						
T	air temperature		×						
p	local air pressure						×		

Table 1 : Data input for solar models

8. COMPARISON OF ORIGINAL SOLAR MODELS

8.1. Correlation of diffuse radiation

The first data set (2007, 2008) was used for the comparison of models. With the respect to the correlation between calculated and measured diffuse radiation were assessed selected models according to their accuracy. The correlation evaluation is based on relative error (RE), mean square deviation (MDS), root means square deviation (RMDS).

For the comparison were included values in the interval 50-1100 $W.m^{-2}$

Figure 2 shows the correlation between the values of diffuse radiation measured by pyranomether and the values computationally derived from the Erb´s solar model. In the total of about 30 261 pairs of measured and predicted diffuse radiation values were used to determine the correlation. The correlation coefficient of their linear regression is defined as 0,69.

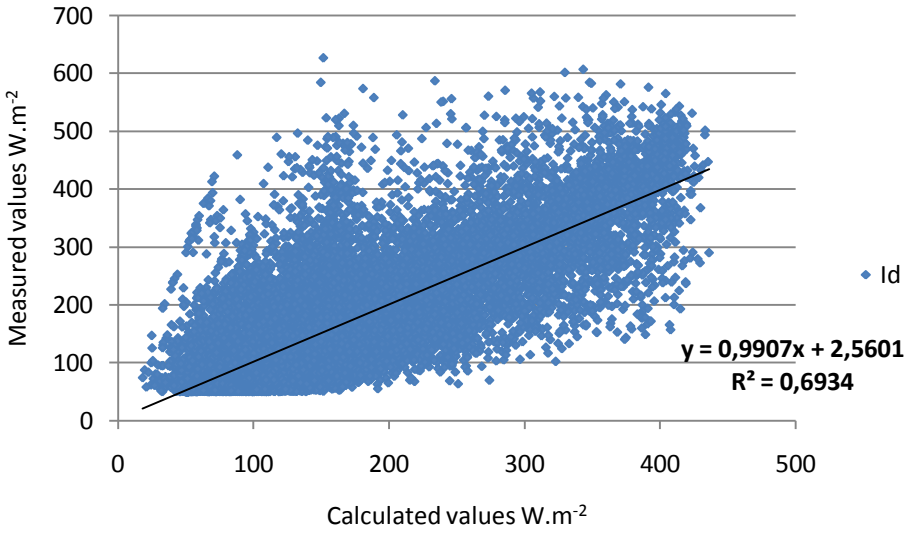

Figure 2 : Correlation between the values measured (I_d) and derived by Erb´s model

Computationally derived values of diffuse radiation by Reindl model are compared with measured diffuse irradiance values based on correlation. A total of about 29 800 pairs of measured-predicted diffuse irradiance values were used to determine the correlation coefficient 0,74 .

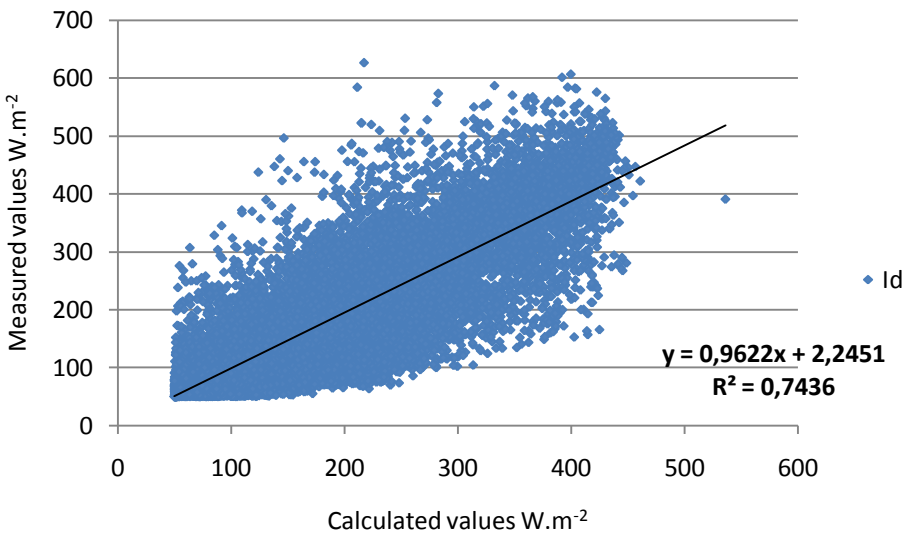

Figure 3 : Correlation between the values measured (I_d) and derived by Reindl´s model

Figure 4 shows computationally derived values of diffuse radiation by Lam and Li model are compared with measured diffuse irradiance values based on correlation. A total of about 30 261 pairs of measured-predicted diffuse irradiance values were used to determine the correlation coefficient 0,63.

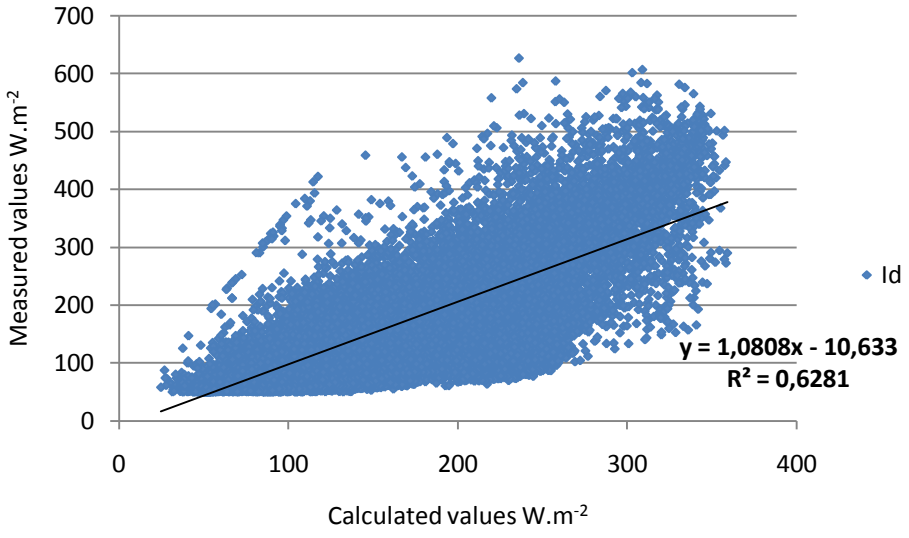

Figure 4 : Correlation between the values measured (I_d) and derived by Lam and Li´s model

Figure 5 illustrates the correlation between the values of diffuse radiation measured by pyranomether and the values computationally derived from the Orgill and Hollands model. In the total of about 30 261 pairs of measured and predicted diffuse radiation values were used to determine the correlation. The correlation coefficient of their linear regression is defined as 0,68.

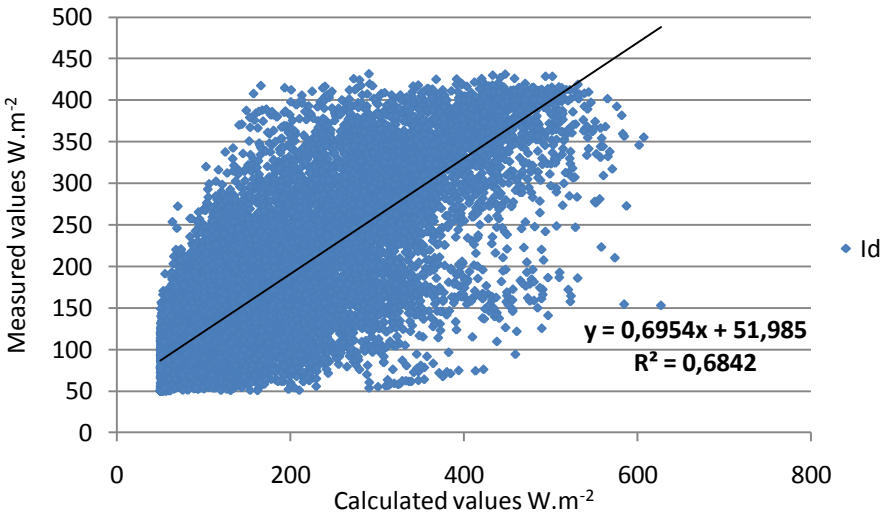

Figure 5 : Correlation between the values measured (I_d) and derived by Orgill and Holland´s model

Figure 6 illustrates the correlation between the values of diffuse radiation measured by pyranomether and the values computationally derived from Skartveit and Olseth model. In the total of about 24 627 pairs of measured and predicted diffuse radiation values were used to determine the correlation. The correlation coefficient of their linear regression is defined as 0,05 .

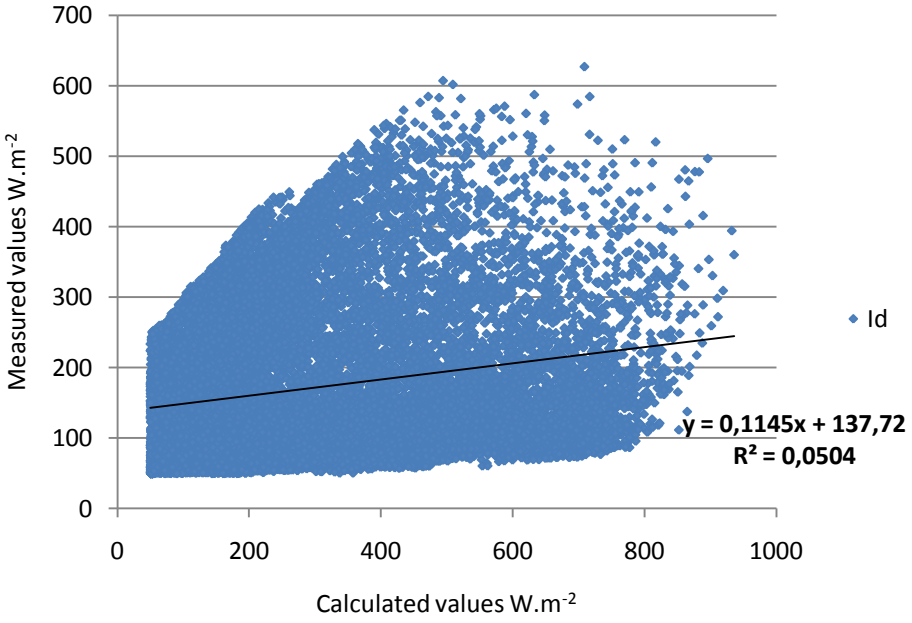

Figure 6 : Correlation between the values measured (I_d) and derived by Skartveit and Olseths model

Figure 7 shows computationally derived values of diffuse radiation by Louches model are compared with measured diffuse irradiance values based on correlation. A total of about 15 549 pairs of measured-predicted diffuse irradiance values were used to determine the correlation coefficient 0,67.

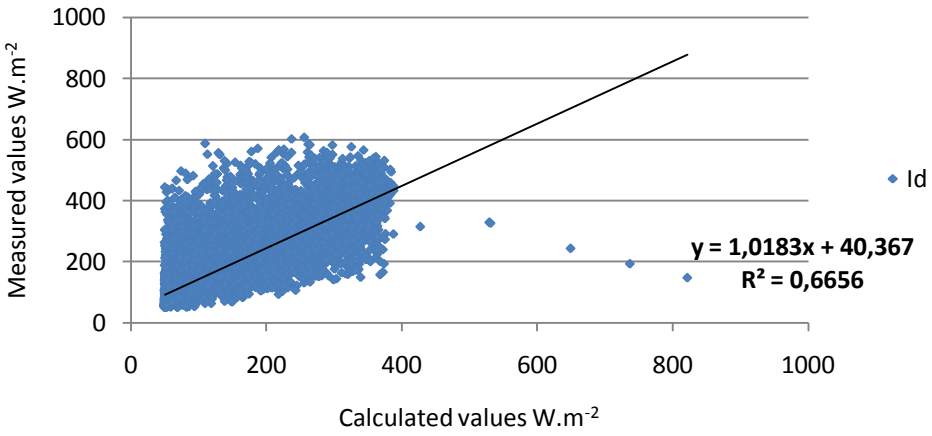

Figure 7 : Correlation between the values measured (I_d) and derived by Louches model

Figure 8 shows computationally derived values of diffuse radiation by Maxwell model are compared with measured diffuse irradiance values based on correlation. A total of about 16 568 pairs of measured-predicted diffuse irradiance values were used to determine the correlation coefficient 0,67.

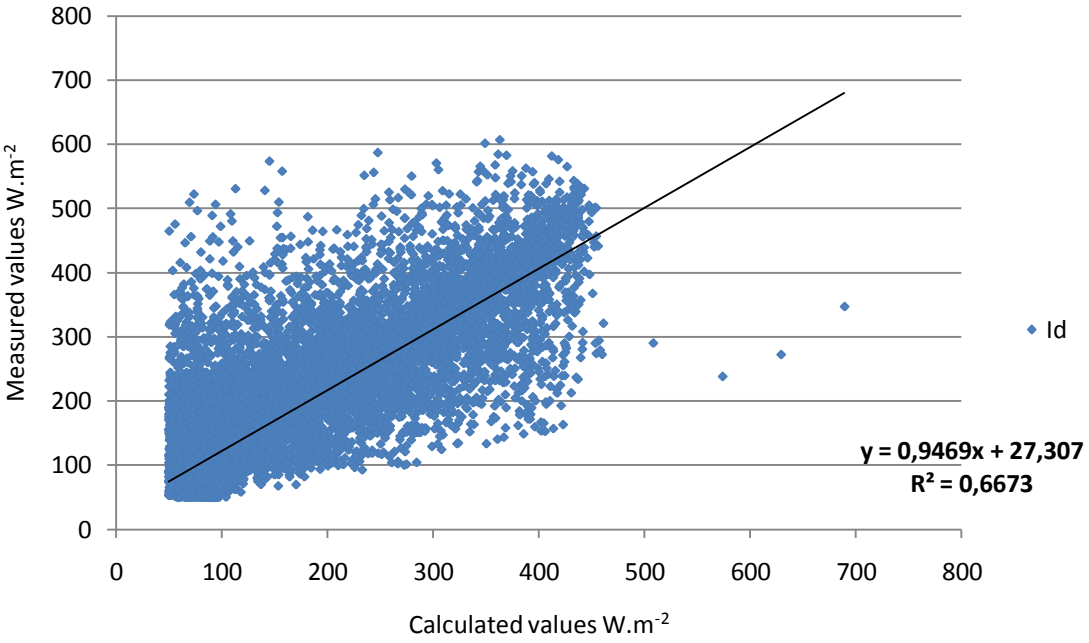

Figure 8 : Correlation between the values measured (I_d) and derived by Maxwell´s model

Figure 9 shows computationally derived values of diffuse radiation by Vignola and McDaniels model are compared with measured diffuse irradiance values based on correlation. A total of about 13 318 pairs of measured-predicted diffuse irradiance values were used to determine the correlation coefficient

.

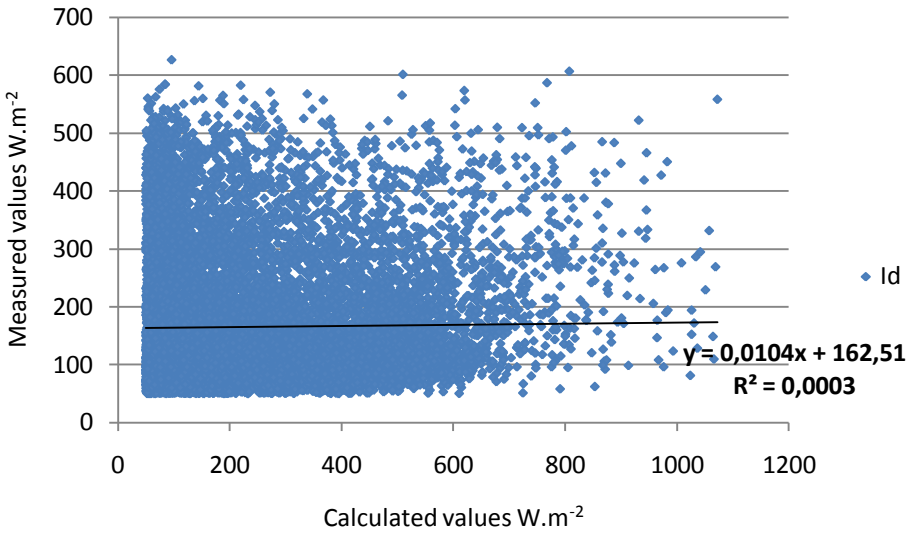

Figure 9 : Correlation between the values measured (I_d) and derived by Vignola and McDaniel´s model

The resulting correlation coefficients (r^2) for all models are summarized in Table 2:

	R^2
Erbs	0,6934
Reindl	0,7436
Lam and Li	0,6281
Orgill and Holand	0,6842
Skartveit and Olseth	0,0504
Louche	0,6656
Maxwell	0,6673
Vignola and McDaniels	0,0003

Table 2 : Correlation coefficients

9. RESULTS OF COMPARISON

Common statistical indicators were used for the comparison of all eight solar models. The relative error between the measurements and predicted derived of diffuse radiation for each model is shown by the Figure 11, for Reind´s models is shown by Figure 10. For the estimation of relative error was used the following equation:

$$\boldsymbol{RE_i = \frac{(M_i - C_i)}{M_i} \cdot 100} \quad [\%]$$

The results of the mean bias difference MBD and relative root mean square difference RMSD, calculated by following equations, can be seen in the Table 3.

$$MBD = \frac{\sum_{i=1}^{n}(M_i - C_i)}{n} \quad [\%]$$

$$RMSD = \frac{\sum_{i=1}^{n}[(M_i - C_i/M_i)]^2}{n} \cdot 100 \quad [\%]$$

where

M_i measured diffuse irradiance (W m^{-2})

C_i computed diffuse irradiance (W m^{-2})

n total number of pairs of diffuse irradiance

9.1. Comparison of Reindl´s solar models

Comparison of three different versions of Reindl´s solar model is expressed by belong chart and table. Exact calculation is described in the chapter 6.2.

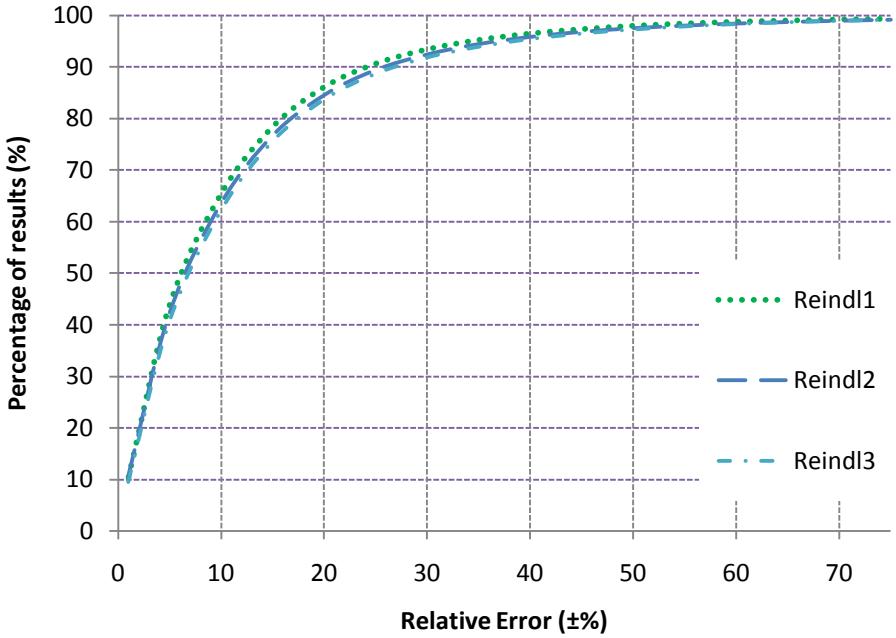

Figure 10 : Relative error of three models of Reindl

The Table 4 compares the three versions of Reindl´s model in the terms of RMSD and MBD for original coefficients of equations.

	MBD	RMBD
Reindl 1	***31,50***	***37,38***
Reindl 2	34,13	42,40
Reindl 3	35,50	40,40

Table 4 : Reindl model characteristics

According to this evaluation was decided to use model Reindl 1 for following work. Model Reindl 1, that include relative humidity and air temperature performed proper calculated results compare to the measurement.

9.2. Comparison of eight solar models

The relative error between the measurements and predicted derived of diffuse radiation for each model is shown by the Figure 11.

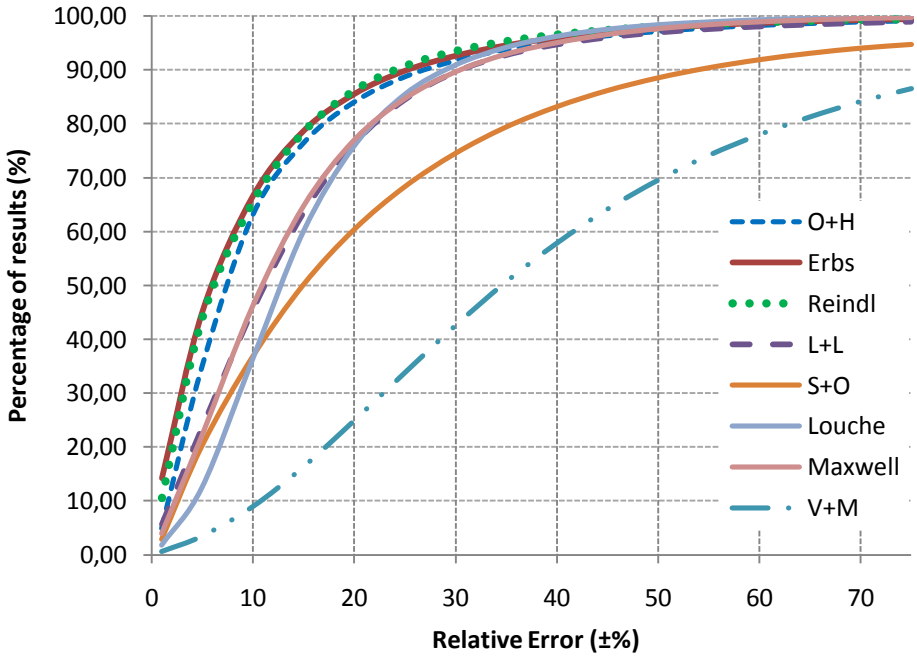

Figure 11 : Percentage of the results with maximum Relative Error for the eight models with original coefficients

The Table 5 compares the eight models in the terms of RMSD and MBD for original coefficients. Results are expressed in percentage.

%	MBD	RMDS
Erbs	32,55	37,43
Reindl	31,50	37,38
Lam and Li	41,8	45,67
Orgill and Holland	35,09	43,09
Skartveit and Olseth	154,32	199,91
Louche	48,87	29,63
Maxwell	42,53	33,22
Vignola and McDaniels	183,08	208,07

Table 5 : Models characteristics

According to this evaluation was decided to use model Erbs, Reindl 1, Lam and Li and Orgill and Holland for creating own model for Vienna data.

10. ADAPTATION OF SOLAR MODELS

Models with the highest accuracy were selected for validation and modification for Vienna weather condition. For the modification and calculation was used second data set (2007, 2008) for Vienna. The average deviation (MBD) between measured and calculated diffuse fraction was determinate by relation:

$$MBD = \sum |k_{d(c)} - k_{d(m)}|/n$$

$k_{d(c)}$ calculated diffuse fraction (-)
$k_{d(m)}$ measured diffuse fraction (-)
n number of pairs (-)
Δ average deviation (-)

The coefficients of equation for each model were modified by the mathematic software MATLAB. The Erbs model was also modified in the statistical software R that provides same results like Matlab.

For the coefficients modification is used mathematic method – linear regression.

The mathematical explanation [2] :

Setting this gradient to zero gives

$$0 = \sum_{n=1}^{N} t_n \, \phi(x_n)^T - w^T \left(\sum_{n=1}^{N} \phi(x_n) \phi(x_n)^T \right)$$

Solving for *w* we obtain

$$w_{ML} = (\phi^{\mathrm{T}}\phi)^{-1}\phi^{\mathrm{T}} t$$

which are known as the *normal equations* for the least squares problem. Here Φ is an N ×M matrix, called the *design matrix*, whose elements are given by $\Phi_{nj} = \Phi_j (x_n)$,

so that

$$\phi = \begin{pmatrix} \phi_0(x_1) & \phi_1(x_1) \dots & \phi_{M-1}(x_1) \\ \phi_0(x_2) & \phi_1(x_2) \dots & \phi_{M-1}(x_2) \\ \vdots & \vdots & \vdots \\ \phi_0(x_N) & \phi_1(x_N) \dots & \phi_{M-1}(x_N) \end{pmatrix}$$

The quantity

$$\phi \equiv (\phi^{\mathrm{T}}\phi)^{-1}\phi^{\mathrm{T}}$$

10.1. Modification of Erb´s model

The original equation:

$$k_d = 1 - 0{,}09k_t \;\; ; \;\; k_t \leq 0{,}22$$

$$k_d = 0{,}9511 - 0{,}1604k_t \;\; + 4{,}388k_t^2 - 16{,}638k_t^3 + 12{,}336k_t^4; \;\; 0{,}22 < k_t \leq 0{,}8$$

$$k_d = 0{,}165 \qquad ; \;\; k_t > 0{,}8$$

k_t clearness index (-)
k_d diffuse fraction (-)

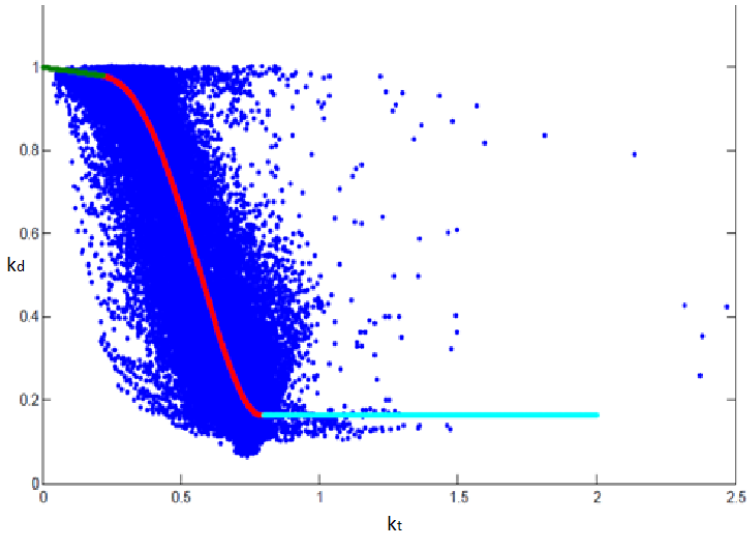

Figure 12 : Relation between k_t and k_d; trend line of original equations for Erbs model

Measured data are described by the relation between k_t (clearness index) and k_d (diffuse fraction). The coloured curves describe graphically each equation of Erbs model. The average deviation between measured and calculated diffuse fraction is 0,105.

The modified equation:

$$k_d = 1 - 0{,}2170k_t \;\; ; \;\; k_t \leq 0{,}27$$

$$k_d = -0{,}0011 + 8{,}9975k_t \;\; - 27{,}1462k_t^2 + 27{,}4096k_t^3 - 8{,}9132k_t^4;$$

$$0{,}27 < k_t \leq 0{,}8$$

$$k_d = 0{,}32644 - 0{,}1503k_t \;\; ; \;\; k_t > 0{,}8$$

k_t clearness index (-)
k_d diffuse fraction (-)

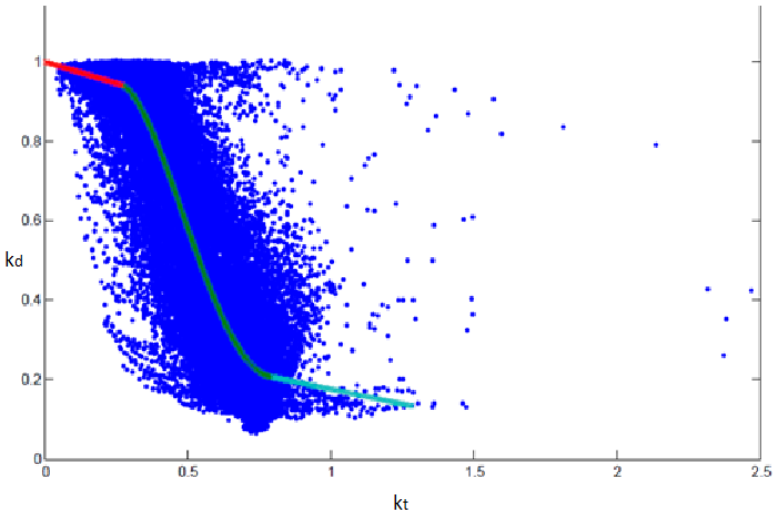

Figure 13 : Relation between k_t and k_d; trend line of original equations for Erbs model

It was aligned the trend line for each interval. Middle interval was modelled by the polynomial of 4^{th} order. The other two intervals were approximated by linear function to fit the data.

Measured data are described by the relation between k_t (clearness index) and k_d (diffuse fraction). The coloured curves describe graphically each equation of modified Erbs model. The average deviation between measured and calculated diffuse fraction is 0,092.

10.2. Modification of Reindl´s model

The original equation:

Interval : $0 \leq k_t \leq 0{,}3$ Constraint : $I_d/I_t \leq 1{,}0$

$$k_d = 1{,}000 - 0{,}232k_t + 0{,}0239\sin\alpha - 0{,}000682T_a + 0{,}0195\Phi$$

Interval : $0{,}3 < k_t < 0{,}78$ Constraint : $0{,}1 \leq I_d/I_t \leq 0{,}97$

$$k_d = 1{,}329 - 1{,}716k_t + 0{,}267\sin\alpha - 0{,}00357T_a + 0{,}106\Phi$$

Interval : $k_t \geq 0{,}78$ Constraint : $I_d/I_t \geq 0{,}1$

$$k_d = 0{,}426k_t - 0{,}256\sin\alpha + 0{,}00349T_a + 0{,}0734\Phi$$

k_t clearness index (-)
k_d diffuse fraction (-)

The projection of the 5D data of the function *y=f(x1, x2, x3, x4)*. The red cloud of point describes the relation between measured values of k_t and k_d. Green points in the graph are calculated values of k_d, that depend on four input variables (k_t, α, T_a, ϕ). The argument fixation cannot be used, therefore we get the "cloud" of data points instead of simple trend line.

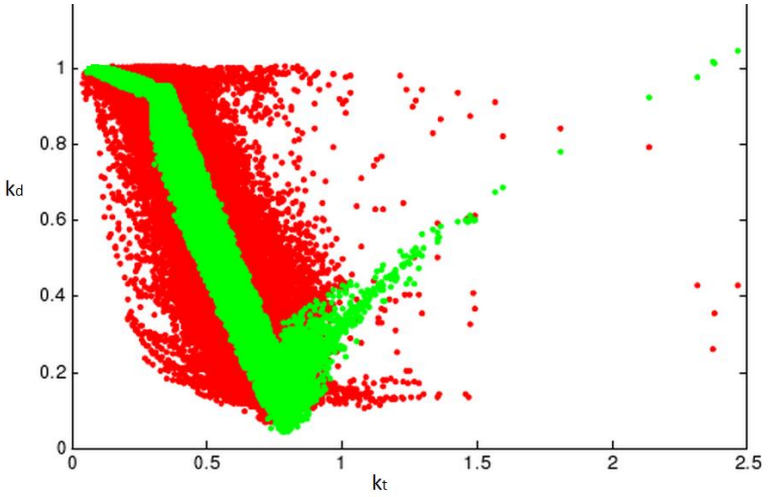

Figure 14 : Overlap of the red measured data (red cloud) and original equation of the Reindls model (green cloud)

The average deviation between measured and calculated diffuse fraction is 0,099.

Derivation of diffuse irradiance based on measured global irradiance data

The modified equation:

Interval : $0 \leq k_t \leq 0{,}3$ Constraint : $I_d/I_t \leq 1{,}0$

$$k_d = 0{,}9369 - 0{,}1809k_t + 0{,}0476\sin\alpha - 0{,}0019T_a + 0{,}0865\Phi$$

Interval : $0{,}3 < k_t < 0{,}78$ Constraint : $0{,}1 \leq I_d/I_t \leq 0{,}97$

$$k_d = 1{,}2158 - 1{,}5545k_t + 0{,}1665\sin\alpha - 0{,}00517T_a + 0{,}2840\Phi$$

Interval : $k_t \geq 0{,}78$ Constraint : $I_d/I_t \geq 0{,}1$

$$k_d = 0{,}4639 - 0{,}1502k_t - 0{,}4136\sin\alpha + 0{,}003T_a + 0{,}3024\Phi$$

Measured data are described by the relation between k_t (clearness index) and k_d (diffuse fraction). The green mesh of points describes each equation of modified Reindls model.

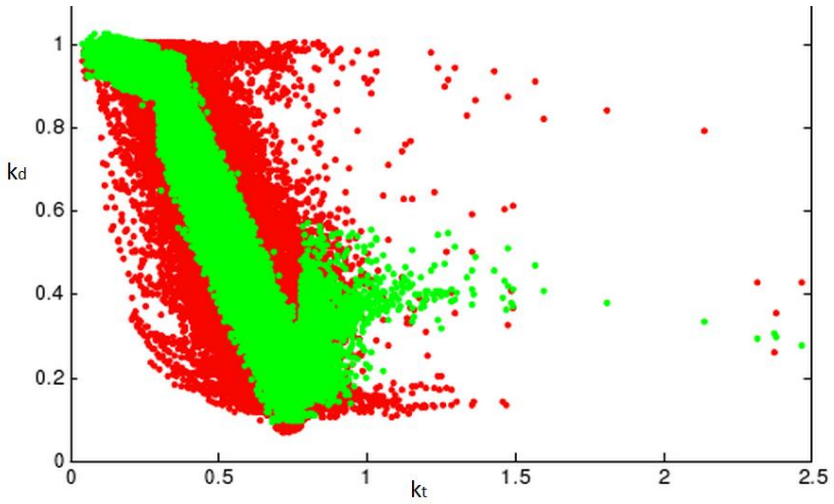

Figure 15 : Overlap of the red measured data (red cloud) and modified (1) equation of the Reindls model (green cloud)

The average deviation between measured and calculated diffuse fraction is 0,101.

The first parameters modification did not have good properties while evaluating on the Vienna data. By further inspection it was discovered that the pairwise correlations between (k_d, sinα), (k_d, ϕ) and (k_d, T_a) are insignificant and introduce noise to the model. Therefore we decided to modify the method in such a way, that we assume that the coefficients a_2, a_3 and a_4 were previously estimated correctly in the original model. Only the a_0, a_1 coefficients are updated. The equation:

$$k_d = a_0 - a_1k_t + a_2\sin\alpha - a_3T_a + a_4\Phi$$

Derivation of diffuse irradiance based on measured global irradiance data

was rewritten in following way:

$$k_d - (a_2 \sin\alpha - a_3 T_a + a_4 \Phi) = a_0 - a_1 k_t \ ,$$

where constant left-hand side term can be marked as k_d':

$$k_d' = a_0 - a_1 k_t \ .\text{x}$$

The estimation of the free parameters a_0 a_1 is then solved by first-order linear regression with single variable, just as is done further in the Lam-Li and Orgill method.

The second modification used original coefficients together with modified coefficients for three variables. The final model, which has modified only two coefficients for each equation (a - constant, b – coefficient of k_t) is described below.

The modified equation with fixed $sin\alpha$, T_a, ϕ:

Interval : $0 \leq k_t \leq 0{,}3$ Constraint : $I_d/I_t \leq 1{,}0$

$$k_d = 0{,}9838 - 0{,}2217 k_t \ + 0{,}0239 \sin\alpha - 0{,}000682 T_a + 0{,}0865 \Phi$$

Interval : $0{,}3 < k_t < 0{,}78$ Constraint : $0{,}1 \leq I_d/I_t \leq 0{,}97$

$$k_d = 1{,}3024 - 1{,}6840 k_t \ + 0{,}267 \sin\alpha - 0{,}00357 T_a + 0{,}106 \Phi$$

Interval : $k_t \geq 0{,}78$ Constraint : $I_d/I_t \geq 0{,}1$

$$k_d = 0{,}4612 - 0{,}0054 k_t \ - 0{,}256 \sin\alpha + 0{,}00349 T_a + 0{,}0734 \Phi$$

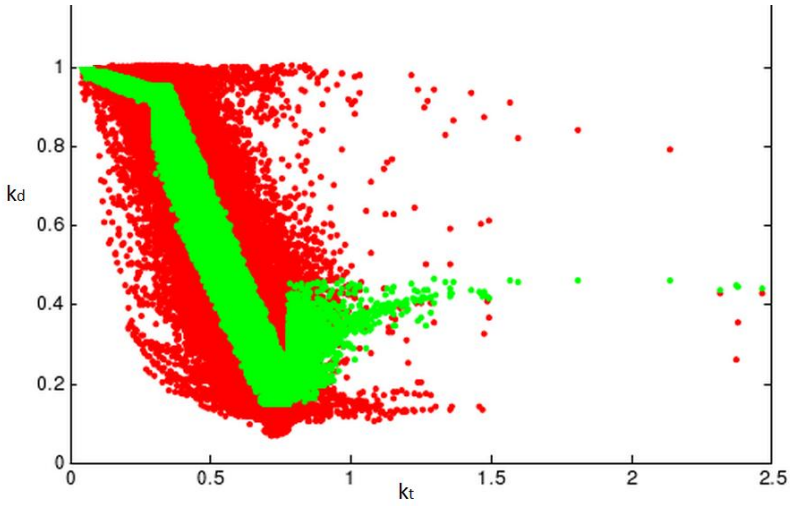

Figure 16 : Overlap of the red measured data (red cloud) and modified (2) equation of the Reindls model (green cloud)

The average deviation between measured and calculated diffuse fraction is 0,087.

This second modified model calculation was used for the future comparison and work with models.

10.3. Modification of Lam and Li´s model

The original equation:

$$k_d = 0{,}977; \quad k_t \leq 0{,}15$$

$$k_d = 1{,}237 - 1{,}361k_t; \quad 0{,}15 < k_t \leq 0{,}7$$

$$k_d = 0{,}273 \quad ; \quad k_t > 0{,}7$$

k_t clearness index (-)
k_d diffuse fraction (-)

The modified equation:

$$k_d = 0{,}9599; \quad k_t \leq 0{,}24$$

$$k_d = 1{,}4178 - 1{,}6685k_t; \quad 0{,}24 < k_t \leq 0{,}73$$

$$k_d = 0{,}2386 \quad ; \quad k_t > 0{,}73$$

k_t clearness index (-)
k_d diffuse fraction (-)

Measured data are described by the relation between k_t (clearness index) and k_d (diffuse fraction). The coloured curves describe graphically each equation of original Lam and Li model. The average deviation between measured and calculated diffuse fraction is 0,119.

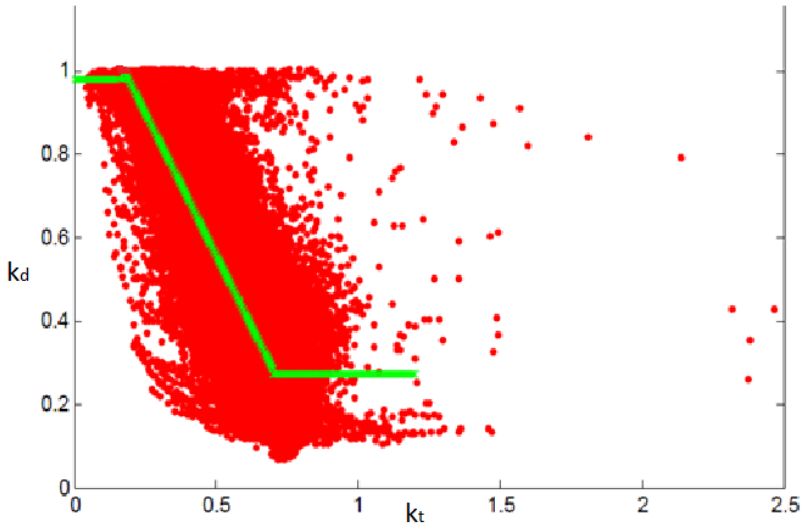

Figure 17 : Relation between k_t and k_d; trend line of original equations for Lam and Li model

Measured data are described by the relation between k_t (clearness index) and k_d (diffuse fraction). The coloured curves describe graphically each equation of modified Lam and Li model. The average deviation between measured and calculated diffuse fraction is 0,097.

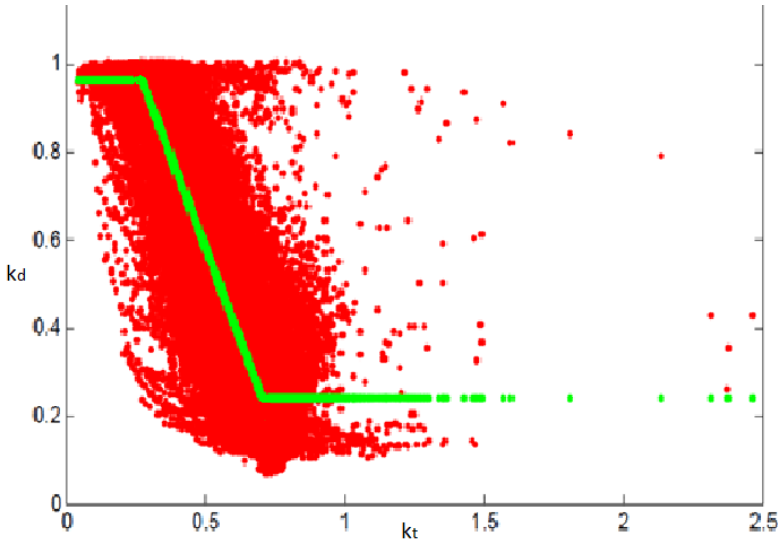

Figure 18 : Relation between data and modified equations of model Lam and Li

Derivation of diffuse irradiance based on measured global irradiance data

10.4. Modification of Orgill and Holland´s model

The original equation:

$$k_d = 1 - 0{,}249k_t \;\; ; \;\; k_t < 0{,}35$$

$$k_d = 1{,}577 - 1{,}84k_t \;\; ; \;\; 0{,}35 <\leq k_t \leq 0{,}75$$

$$k_d = 0{,}177 \qquad ; \;\; k_t > 0{,}75$$

k_t clearness index (-)
k_d diffuse fraction (-)

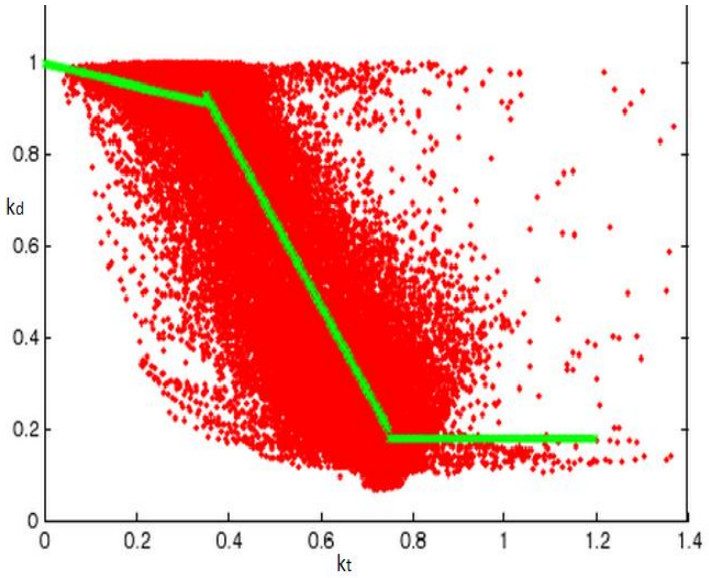

Figure 19 : Relation between data and original equations of model Orgill and Holland

Measured data are described by the relation between k_t (clearness index) and k_d (diffuse fraction). The coloured curves describe graphically each equation of original Orgill and Hollands model. The average deviation between measured and calculated diffuse fraction is 0,11.

Derivation of diffuse irradiance based on measured global irradiance data

The modified equation:

$$k_d = 1 - 0{,}149k_t \;\; ; \;\; k_t < 0{,}35$$

$$k_d = 1{,}47 - 1{,}761k_t \;\; ; \;\; 0{,}35 <\leq k_t \leq 0{,}75$$

$$k_d = 0{,}182 \;\; ; \;\; k_t > 0{,}75$$

k_t clearness index (-)
k_d diffuse fraction (-)

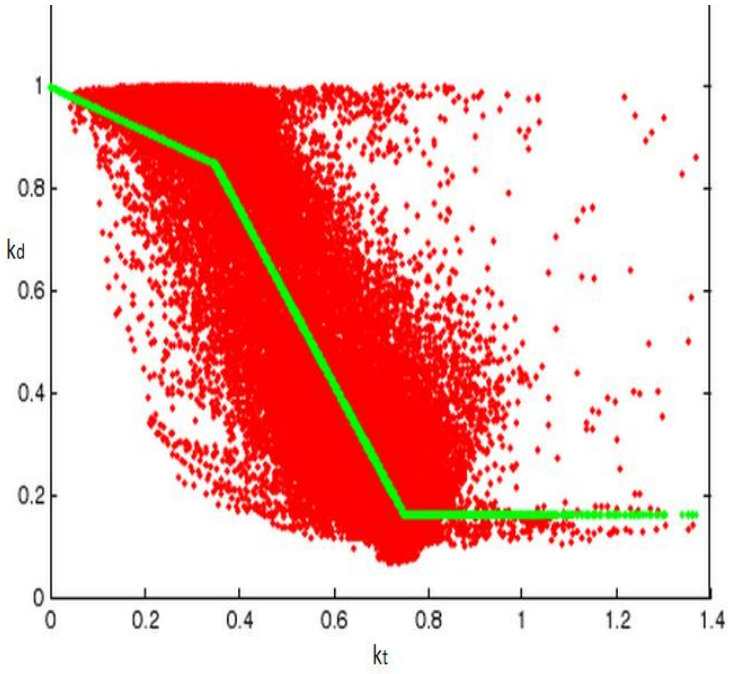

Figure 20 : Relation between data and modified equations of model Orgill and Holland´s

Measured data are described by the relation between k_t (clearness index) and k_d (diffuse fraction). The coloured curves describe graphically each equation of modified Orgill and Hollands model. The average deviation between measured and calculated diffuse fraction is 0,089.

11. COMPARISON OF MODIFIED SOLAR MODELS

11.1. Correlation of diffuse radiation for modified models

Modified models (Erbs, Reindl, Lam and Li. Orgill and Holland) were used for the calculation of diffuse radiation based on first data (2007, 2008) set. For comparison was used second data set (2008, 2009, 2010). For the comparison were included values in the interval 50-1100 $W.m^{-2}$.

Figure 21 shows computationally derived values of diffuse radiation by modified Erbs model are compared with measured diffuse irradiance values based on correlation. A total of about 30 663 pairs of measured-predicted diffuse irradiance values were used to determine the correlation coefficient.

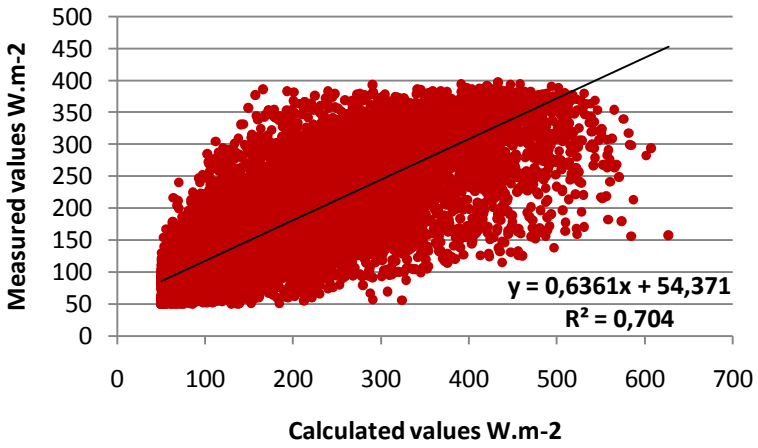

Figure 21 : Correlation between the values (I_d) measured and derived by modified Erb´s model

Computationally derived values of diffuse radiation by modified Reindl´s model are compared with measured diffuse irradiance values based on correlation.
A total of about 29 645 pairs of measured-predicted diffuse irradiance values were used to determine the correlation coefficient 0,76.

Derivation of diffuse irradiance based on measured global irradiance data

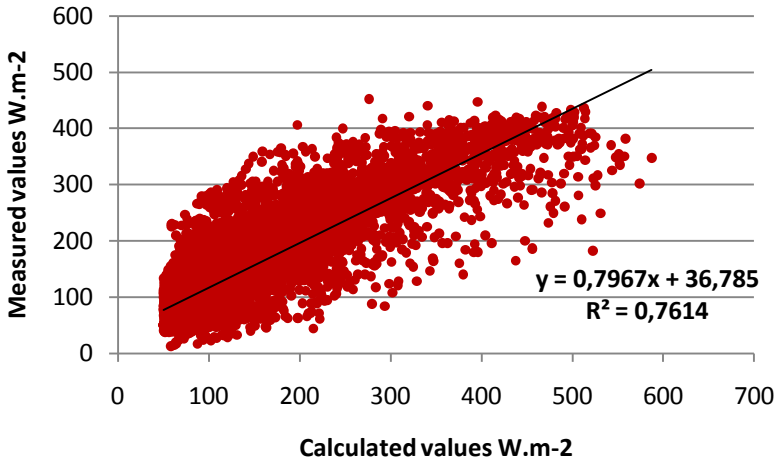

Figure 22 : Correlation between the values (I_d) measured and derived by modified Reindl´s model

Computationally derived values of diffuse radiation by modified Lam and Li model are compared with measured diffuse irradiance values based on correlation. A total of about 30 055 pairs of measured-predicted diffuse irradiance values were used to determine the correlation coefficient 0,68.

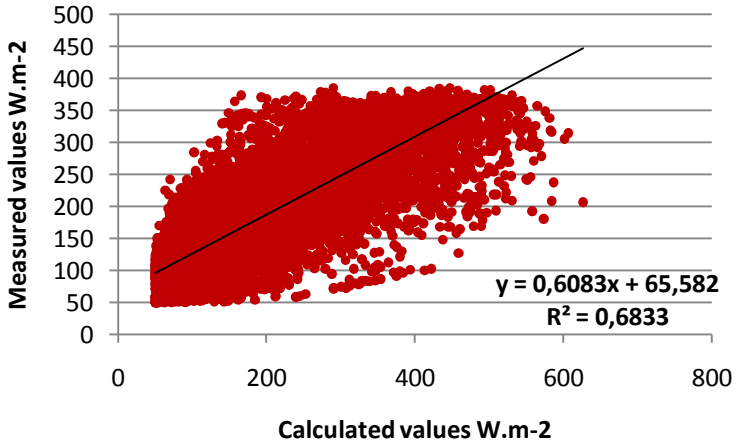

Figure 23 : Correlation between the values measured (I_d) and derived by modified Lam and Li´s model

Computationally derived values of diffuse radiation by modified Orgill and Holland model are compared with measured diffuse irradiance values based on correlation. A total of about 30 055 pairs of measured-predicted diffuse irradiance values were used to determine the correlation coefficient 0,698.

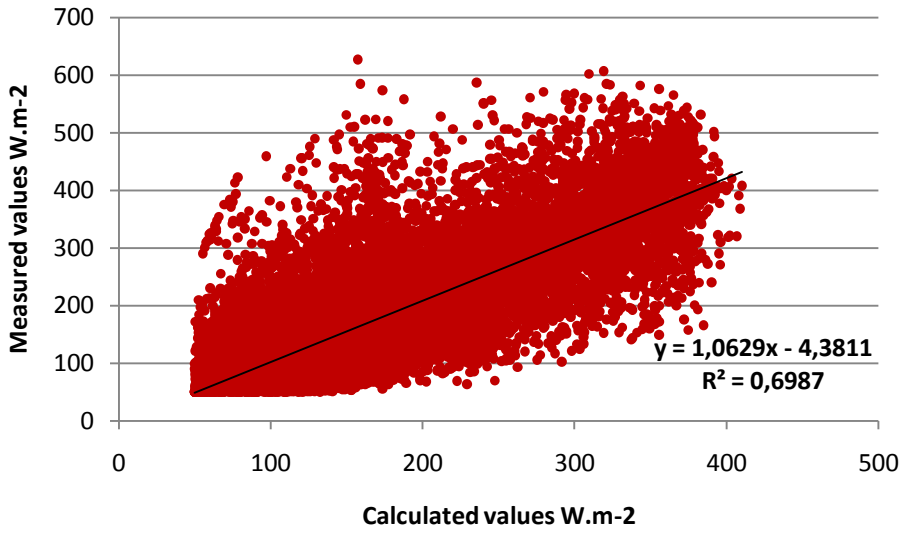

Figure 24 : Correlation between the values measured (I_d) and derived by modified Orgill and Holland´s model

11.1.1. Relative Error for modified models

To compare the performance of the three modified solar models (using the first data set of measurements), the Figure 25 shows the percentage of the results with associated maximum relative errors.

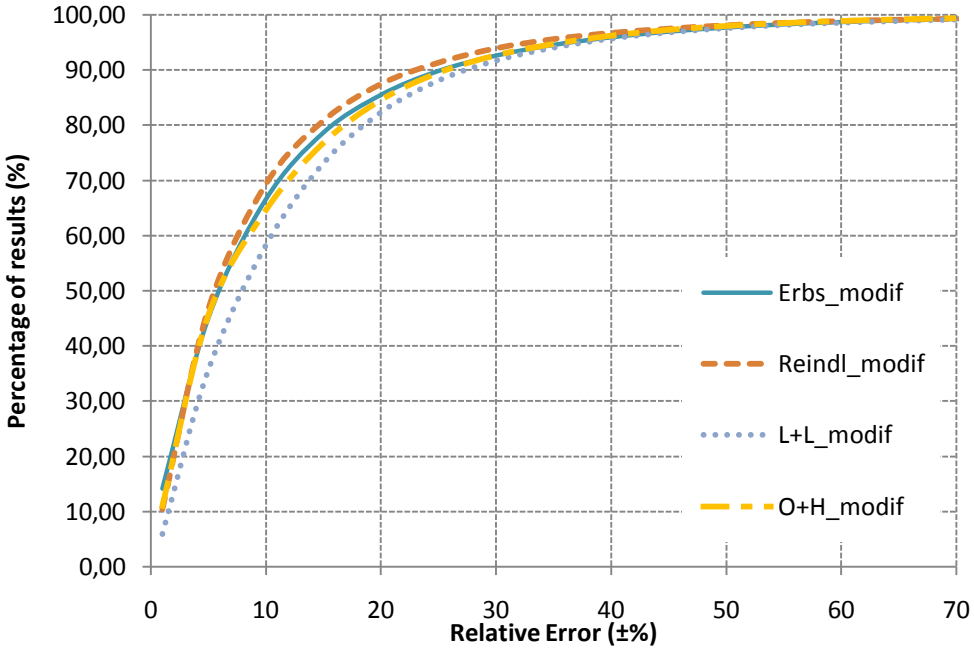

Figure 25 : Relative Error for three models with modified coefficients (2008, 2009,2010)

It is obvious from the Figure 25, that the modified model of Reind provides highest accuracy of the calculation of diffuse radiation compared to the measured values.

12. RESULTS OF COMPARISON OF MODIFIED MODELS

Common statistical indicators were used for the comparison of three modified solar models. The relative error between the measurements and predicted derived of diffuse radiation for each modified model is shown by the Figure 26. For the estimation of relative error was used the equation described in chapter 9:

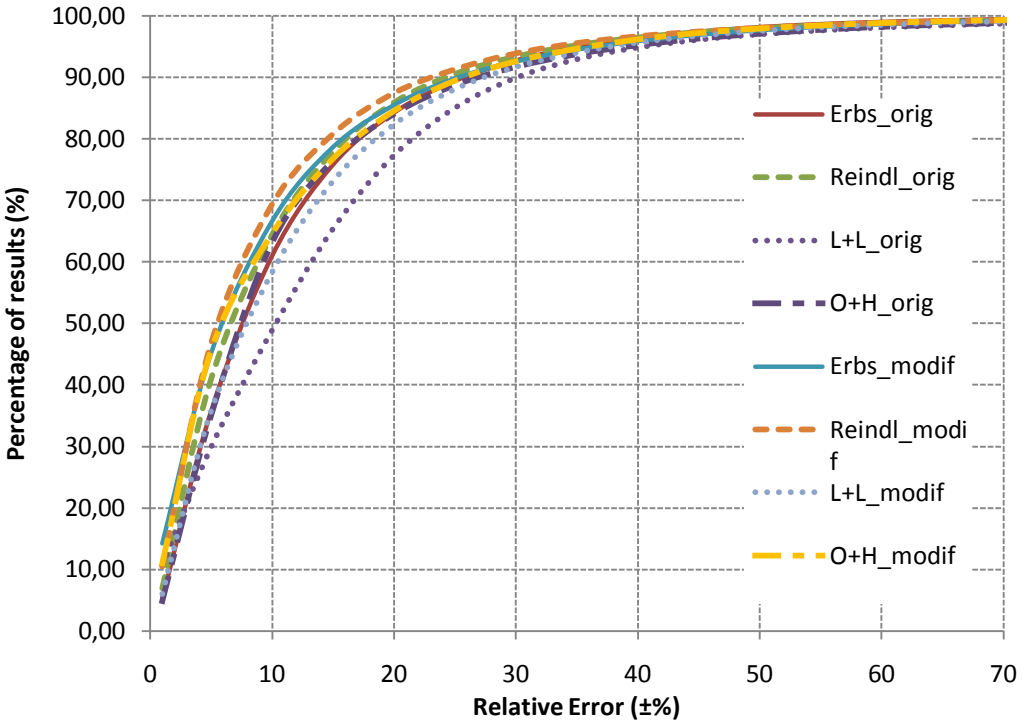

Figure 26 : Percentage of the results with maximum Relative Error for three models with modified and original coefficients (data 2007,2008)

The resulting correlation coefficients (r^2) for all models are summarized in Table 6.

	R^2 orig.	**R^2 modif.**	**MBD k_d (orig)**	**MBD k_d (mod.)**
Erbs	0,6934	0,704	10,5	9,2
Reindl	0,7436	0,7614	9,9	8,7
Lam and Li	0,6281	0,6833	11,9	9,7
Orgill and Holland	0,6842	0,6987	11,1	8,9

Table 6 : Correlation coefficients (2008,2009,2010) and deviation of k_d (2008,2009,2010)

The Table 5 compares the three original and modified models in the terms of RMSD and MBD for original coefficients. Results are expressed in percentage.

%	**MBD orig.**	**RMDS orig.**	**MBD modif.**	**RMDS modif.**
Erbs	32,55	37,43	31,89	33,23
Reindl	31,50	37,38	27,55	36,94
Lam and Li	41,8	45,67	35,66	39,09
Orgill and Holland	35,09	43,09	32,89	34,99

Table 7 : Table of characteristics (2008, 2009, 2010)

12.1. Comparison according to the clearness index intervals

12.1.1. Erb´s model

Erb´s model includes two linear and one polynomial equation. Following comparison provides an overview about the fitting curve to each equation and the accuracy of modified equation in dependence of intervals (sky condition).

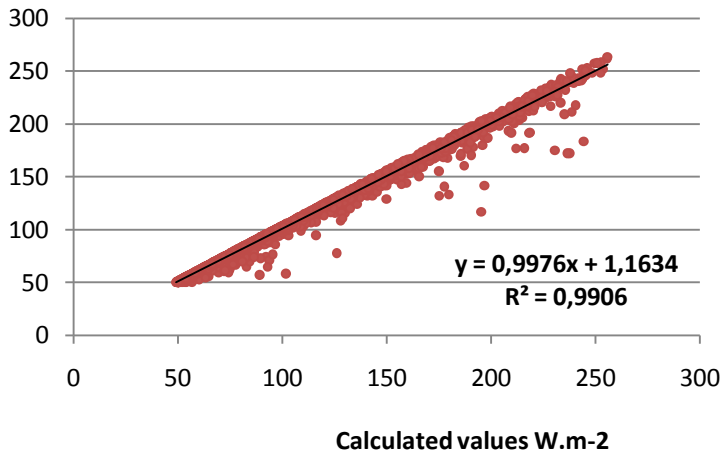

Figure 27 : Correlation between the values measured (I_d) and derived by modified Erb´s model – interval $k_t \leq 0{,}22$ data (2008, 2009, 2010)

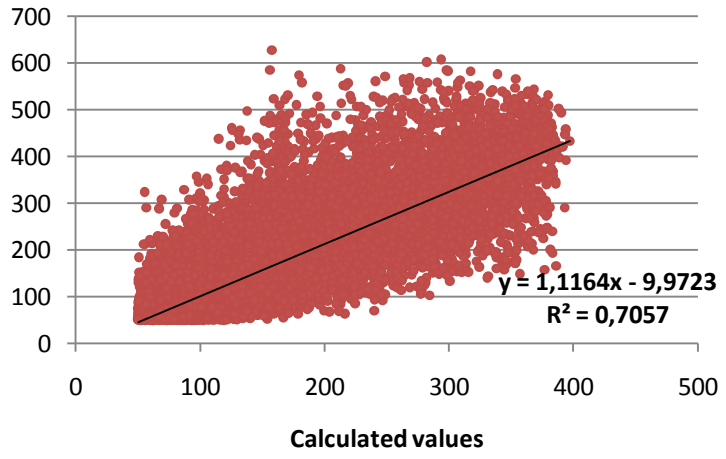

Figure 28 : Correlation between the values measured (I_d) and derived by modified Erb´s model – interval $0{,}22 < k_t \leq 0{,}8$ data (2008, 2009, 2010)

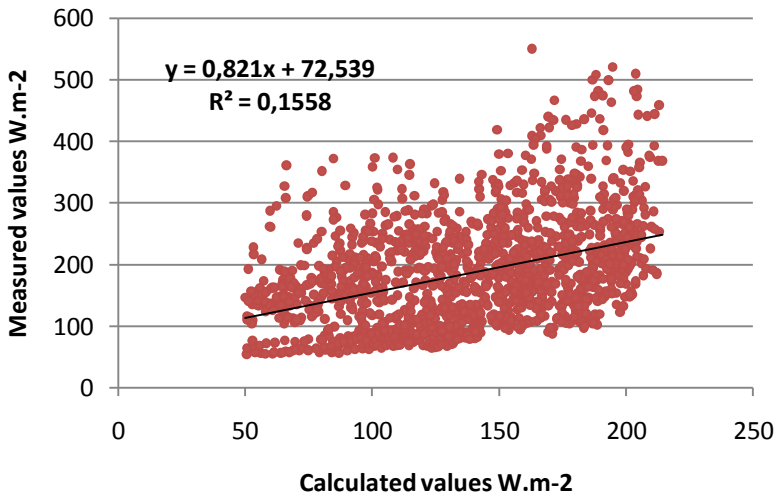

Figure 29 : Correlation between the values measured (Id) and derived by modified Erb´s model – interval k_t>0,8 data (2008, 2009, 2010)

A total of about 7 128 pairs of measured-predicted diffuse irradiance values were used to determine the correlation coefficient 0,99 in the interval $k_t \leq 0,22$. The interval $0,22 < k_t \leq 0,8$ is represented by 28 338 pairs of measured and calculated diffuse irradiance value. The correlation coefficient for the middle interval is 0,70. The correlation coefficient for the calculated correlation in the interval k_t>0,8 is 0,15. It was used 1 619 pair of measured values for the calculation.

	R^2 modif.
Erbs, $k_t \leq 0,22$	0,9906
Erbs, $0,22 < k_t \leq 0,8$	0,7057
Erbs, k_t>0,8	0,1558

Table 8 : Correlation coefficients for Erb´s model according to the intervals

12.1.2. Reindl model

Reindl model includes three linear equations with different four input variables (k_t, α, T_a, ϕ). Correlation graphs of each equation for three intervals describe the accuracy of calculation according to the sky condition. (clearness index).

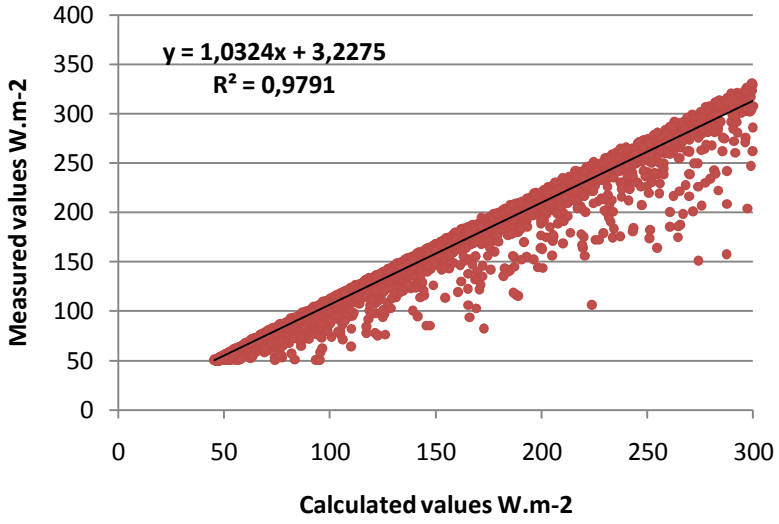

Figure 30 : Correlation between the values measured (I_d) and derived by modified Reindl´s model – interval $k_t \leq 0,3$ data (2008, 2009, 2010)

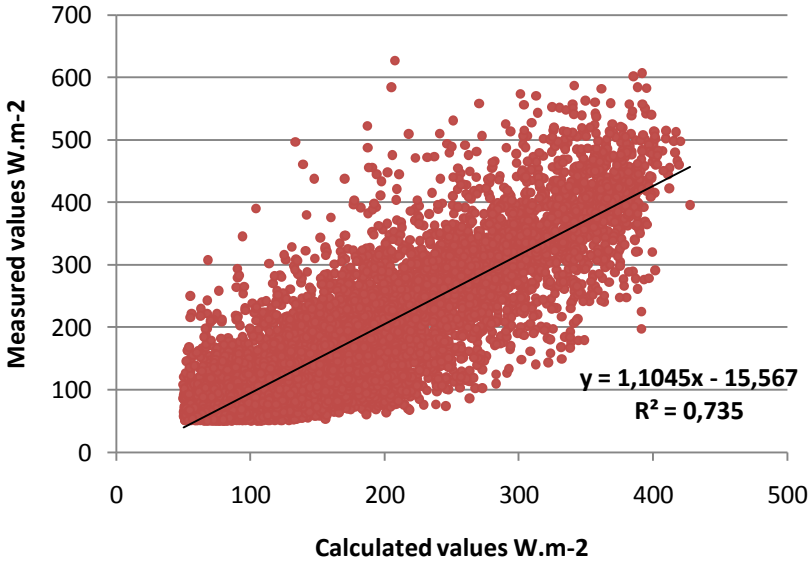

Figure 31 : Correlation between the values measured (I_d) and derived by modified Reindl´s model – interval $0,3 < k_t < 0,78$ data (2008, 2009, 2010)

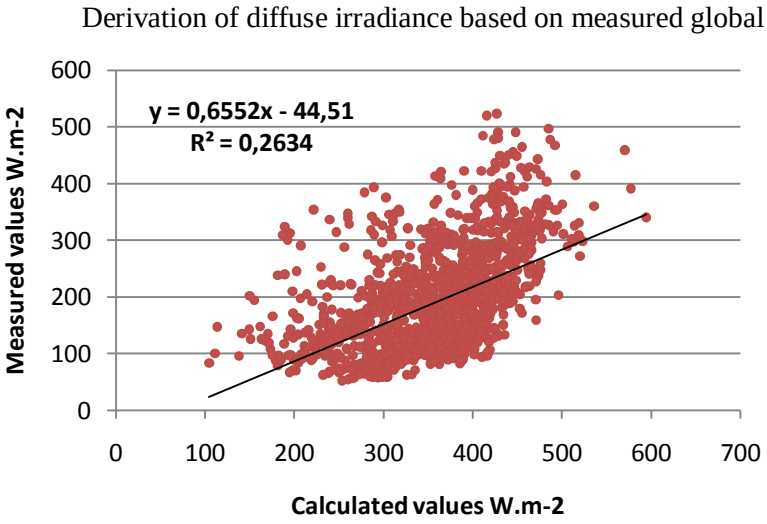

Figure 32 : Correlation between the values measured (I_d) and derived by modified Reindl´s model – interval $k_t \geq 0,78$ data (2008, 2009, 2010)

A total of about 9 009 pairs of measured-predicted diffuse irradiance values were used to determine the correlation coefficient 0,98 in the interval $k_t \leq 0,3$. The interval $0,3 < k_t \leq 0,78$ is represented by 9 999 pairs of measured and calculated diffuse irradiance value. The correlation coefficient for the middle interval is 0,74. The correlation coefficient for the calculated correlation in the interval $k_t \geq 0,78$ is 0,26. It was used 2 289 pair of measured values for the calculation.

	R^2 modif.
Reindl, $k_t \leq 0,3$	0,9791
Reindl, $0,3 < k_t \leq 0,78$	0,735
Reindl, $k_t \geq 0,78$	0,2634

Table 9 : Correlation coefficients for Reindl´s model according to the intervals

12.1.3. Lam and Li model

Lam and Li model includes three linear equations with one input variable (k_t). Correlation graphs of each equation for three intervals describe the accuracy of calculation according to the sky condition. (clearness index).

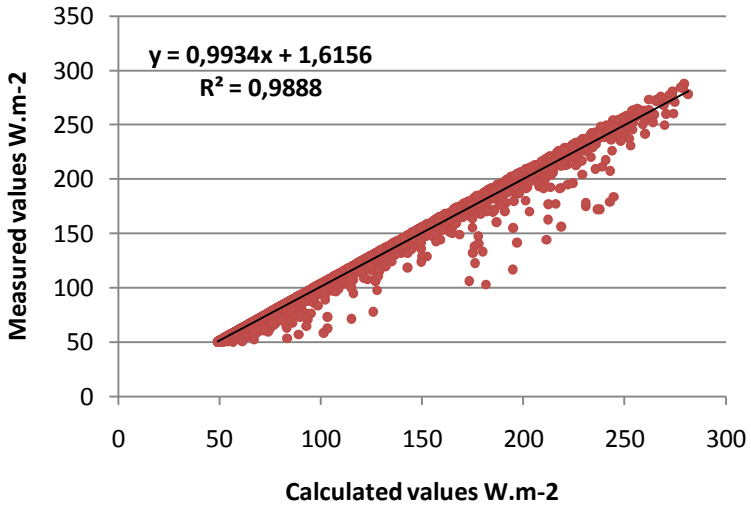

Figure 33 : Correlation between the values measured (I_d) and derived by modified Lam and Li model – interval $k_t \leq 0{,}15$ data (2008, 2009, 2010)

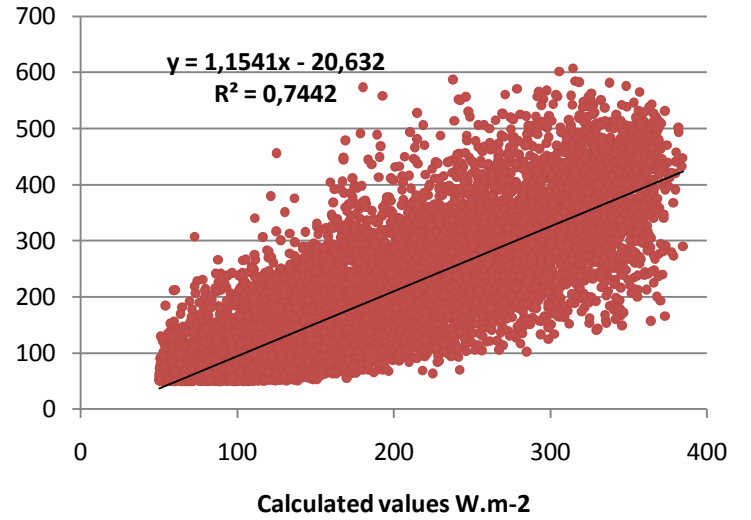

Figure 34 : Correlation between the values measured (I_d) and derived by modified Lam and Li model – interval $0{,}15 < k_t \leq 0{,}7$ data (2008, 2009, 2010)

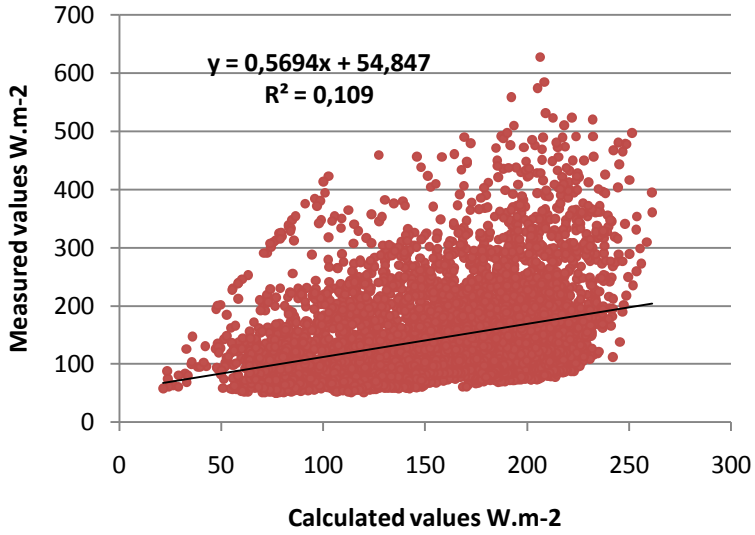

Figure 35 : Correlation between the values measured (I_d) and derived by modified Lam and Li model – interval k_t>0,7 data (2008, 2009, 2010)

A total of about 964 pairs of measured-predicted diffuse irradiance values were used to determine the correlation coefficient 0,99 in the interval $k_t \leq 0,15$. The interval $0,15 < k_t \leq 0,7$ is represented by 23 167 pairs of measured and calculated diffuse irradiance value. The correlation coefficient for the middle interval is 0,74. The correlation coefficient for the calculated correlation in the interval k_t>0,8 is 0,11. It was used 6 130 pair of measured values for the calculation.

	R^2 modif.
Lam and Li, $k_t \leq 0,15$	0,9888
Lam and Li, $0,15 < k_t \leq 0,7$	0,7442
Lam and Li, $k_t \geq 0,7$	0,109

Table 10 : Correlation coefficients for Lam and Li model according to the intervals

12.1.4. Orgill and Holland´s model

Orgill and Holland model includes three linear equations with one input variable (k_t). Correlation graphs of each equation for three intervals describe the accuracy of calculation according to the sky condition. (the clearness index).

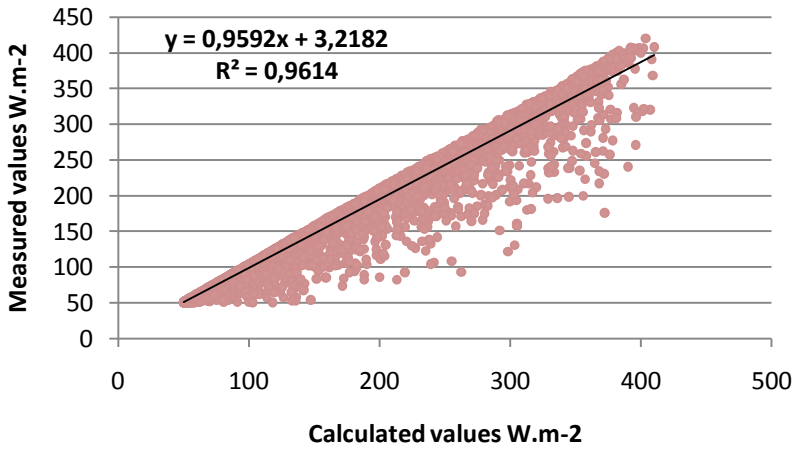

Figure 36 : Correlation between the values measured (I_d) and derived by modified Orgill and Holland´s model – interval k_t<0,35 data (2008, 2009, 2010)

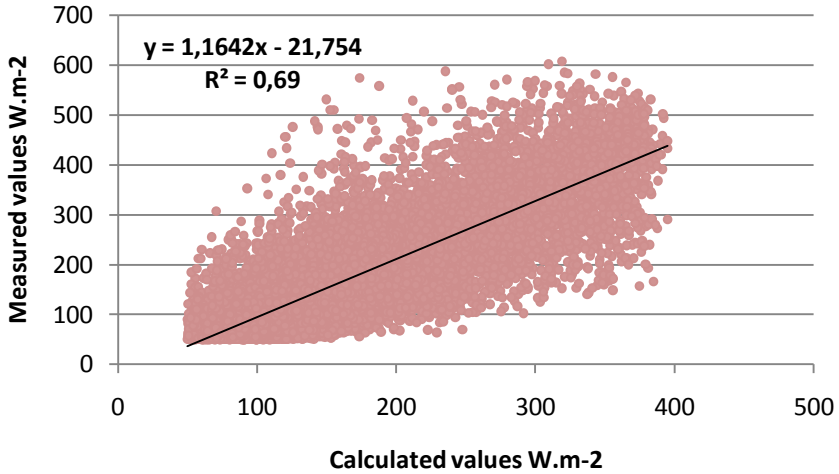

Figure 37 : Correlation between the values measured (I_d) and derived by modified Orgill and Holland´s model – interval 0,35≤k_t≤0,75 data (2008, 2009, 2010)

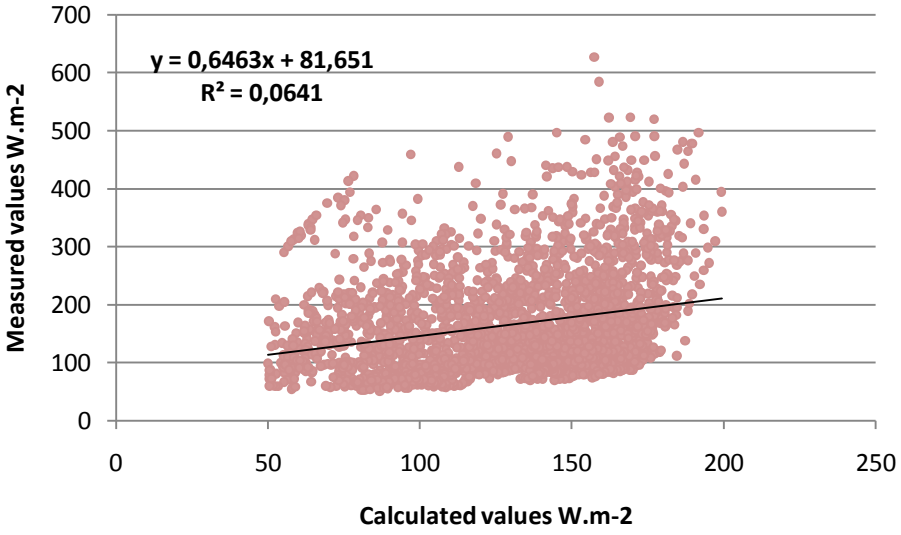

Figure 38 : Correlation between the values measured (I_d) and derived by modified Orgill and Holland´s model – interval k_t>0,75 data (2008, 2009, 2010)

A total of about 10 002 pairs of measured-predicted diffuse irradiance values were used to determine the correlation coefficient 0,9614 in the interval $k_t \leq 0,35$. The interval $0,35 < k_t \leq 0,75$ is represented by 15 456 pairs of measured and calculated diffuse irradiance value. The correlation coefficient for the middle interval is 0,69. The correlation coefficient for the calculated correlation in the interval k_t>0,75 is 0,0641. It was used 2 844 pair of measured values for the calculation.

	R^2 modif.
Orgill and Holland, k_t <0,35	0,9614
Orgill and Holland, $0,35 \leq k_t \leq 0,75$	0,69
Orgill and Holland, k_t>0,75	0,0641

Table 11 : Correlation coefficients for Orgill and Holland´s model according to the intervals

12.1.5. Relative error

To compare the performance of the three modified solar models according to the clearness index intervals (using the first data set of measurements), the following graphs shows the percentage of the results with associated maximum relative errors.

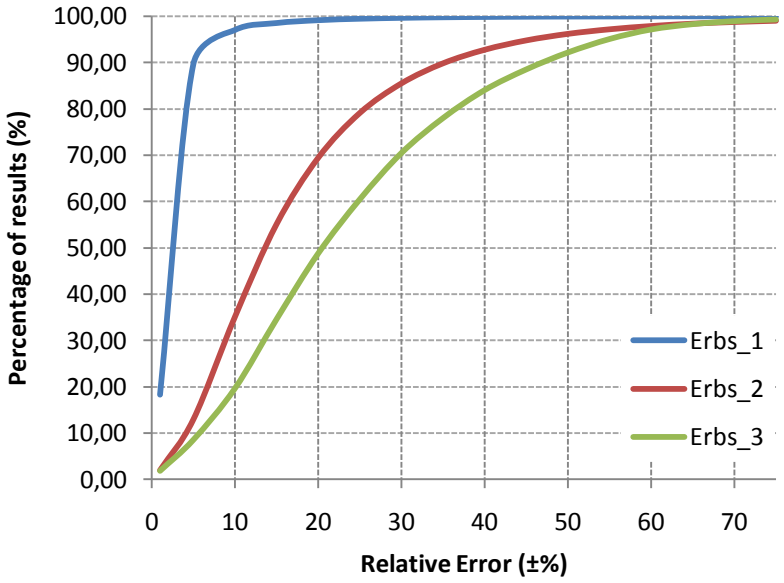

Figure 39 : Relative error according to the different intervals; Erb´s ($k_t \leq 0,22$; $0,22 < k_t \leq 0,8$; $k_t > 0,8$)

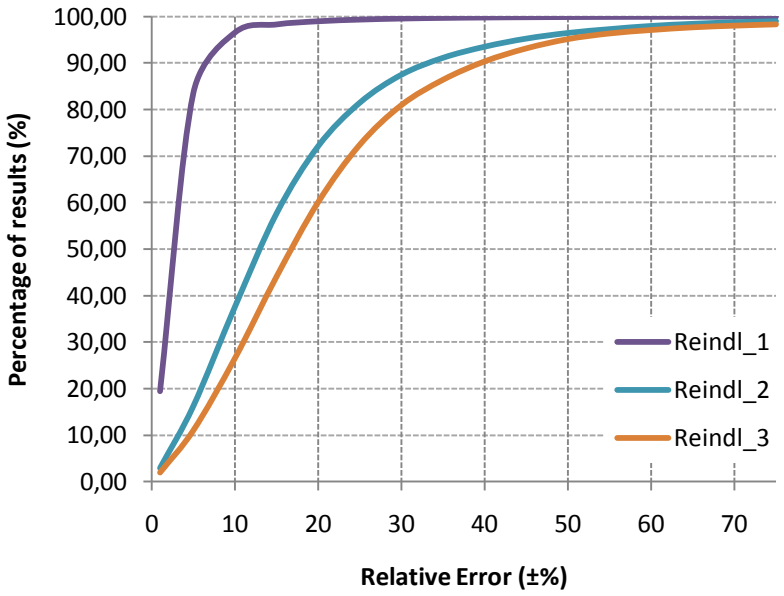

Figure 40 : Relative error according to the different intervals, Reindl´s ($k_t \leq 0,3$; $0,3 < k_t < 0,78$; $k_t \geq 0,78$)

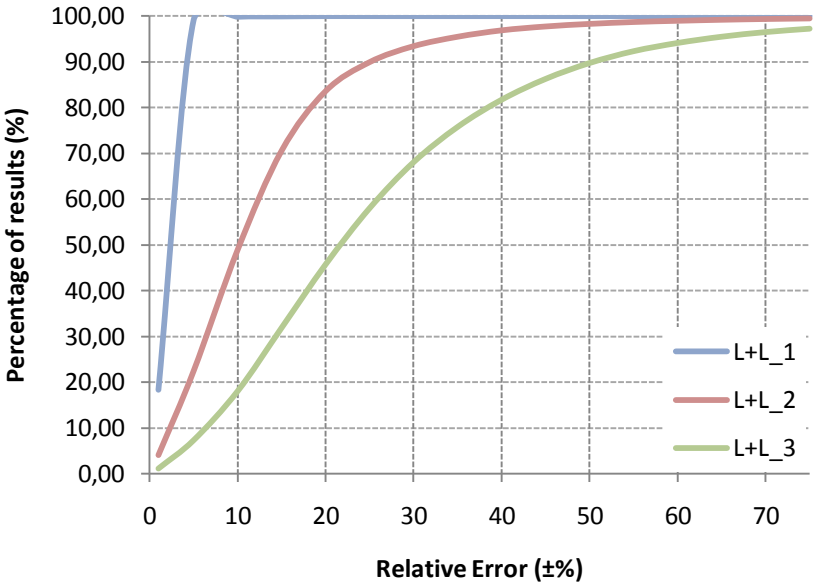

Figure 41 : Relative error according to the different intervals; Lam and Li ($k_t \leq 0,15$; $0,15 < k_t \leq 0,7$; $k_t > 0,7$)

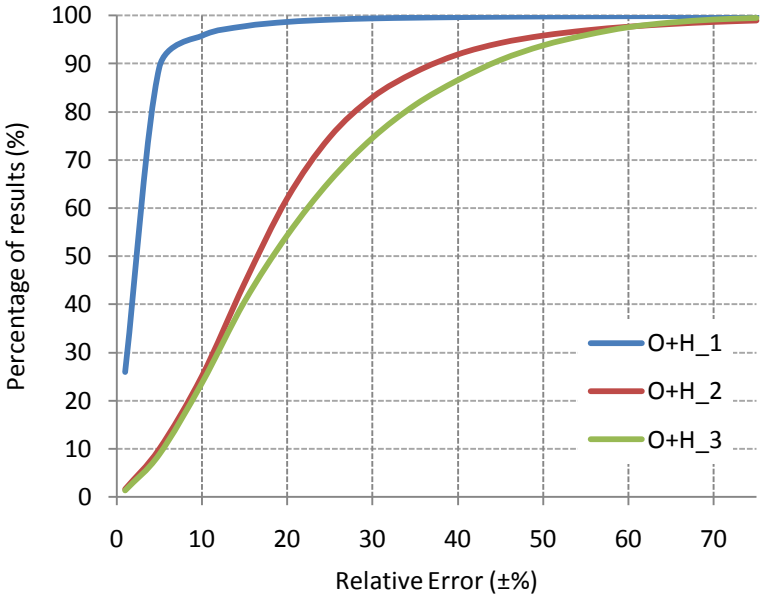

Figure 42 : Relative error according to the different intervals; Orgill and Holland´s ($k_t < 0,35$; $0,35 \leq k_t \leq 0,75$; $k_t > 0,75$)

Comparison of the relative error for each model according to the intervals shows, that the best results are obtained in the interval k_t is lower than 0,3. Clearness index describe the ratio between global and extraterrestrial radiation. Lower value of clearness index shows clear sky – low cloud amount. On the other hand, when the sky is cloudy the results are not proper for all three models.

	R^2 (modif.)	**MDS (modif.)**	**RMDS (modif.)**
Erbs_1	0,99	2,35	3,93
Erbs_2	0,706	36,50	34,70
Erbs_3	0,122	73,49	58,14
Reindl_1	0,979	9,25	8,87
Reindl_2	0,735	35,4	33,5
Reindl_3	0,263	71,04	54,02
L+L_1	0,989	2,84	4,74
L+L_2	0,744	38,11	38,02
L+L_3	0,08	65,49	62,01
O+H _1	0,9614	6,72	12,34
O+H _2	0,69	47,75	44,25
O+H _3	0,0641	62,75	41,93

Table 12 : Table of statistical characteristics data, modified modlels (2008, 2009, 2010)

13. SOLAR MODEL FOR CZECH REPUBLIC

13.1. Measurements of solar radiation in Czech Republic

13.1.1. CHMU

The Czech Hydrometeorological Institute (CHMI) has responsibility for **monitoring of solar radiation in the Czech Republic.** Systematic measurements have been obtained at the CHMI Solar and Ozone Observatory (SOO) in Hradec Kralove, which has been designated as the Czech National Radiation Centre, since the early 1950s. **The network consists of 16 professional meteorological stations** located in typical regions of the Czech Republic (lowlands, highlands, industrial and urban agglomerations, upper parts of the border mountains, etc**.).**

K&Z CM5 and CM11 pyranometers are used for **hourly and daily sums of global and diffuse solar radiation** and are regularly calibrated to the Czech national radiation standard (an Eppley AHF ACR, previously an Angstr`m unit). All data are processed to the international WRR pyrheliometer scale and are stored in the CHMI radiation database at SOO following quality control. For Hradec. [1]

Station	Altitude	Global radiation	Diffuse radiation	Region
	meters	Beginning	Beginning	
České Budějovice	387	I / 2002		LCM1
Churáňov	1122	I / 1984		TM
Doksany	158	VIII / 2003		LCM1
Hradec Králové	285	I / 1964	II / 1964	LCM1
Kocelovice	519	I / 1984		LCM2
Košetice	470	I / 1984	XII / 1995	LCM2
Kuchařovice	334	I / 1984	IX / 1992	LSM
Labská bouda	1320	I / 2006		TM
Luká	510	I / 1984		LCM2
Mošnov	251	XII / 2002		LCM1
Ostrava-Poruba	242	I / 1984		LCM1
Praha-Karlov	254	I / 1984		AP
Praha-Libuš	305	XII / 2003		LCM1
Svratouch	737	I / 1984		HCM
Tušimice	322	V / 1984	XI / 1992	AP
Ústí n. Labem	375	I / 1984		AP

Typical regions:

LCM1	lowlands of Czech and Moravia, altitude up to 400 m
LCM2	lowlands of Czech and Moravia, altitude 400-600 m
LSM	lowlands of South Moravia
HCM	highlands of Czech and Moravia, altitude 600-800 m
TM	top parts of the border mountains
AP	regions of high pollution

Figure 43 : List of stations and periods of monitoring solar radiation in the network of CHMU

[1] http://www.chmu.cz/indexe.html

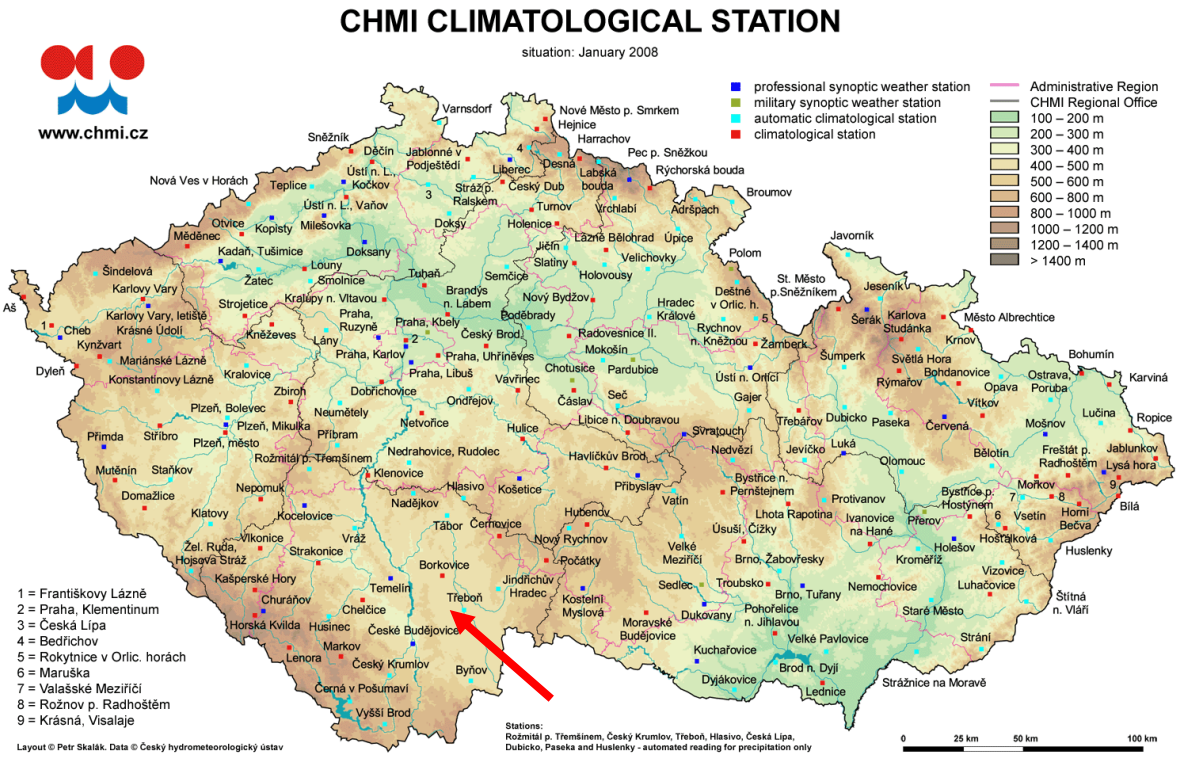

Figure 44 : Map of climatological stations in the network of CHMU

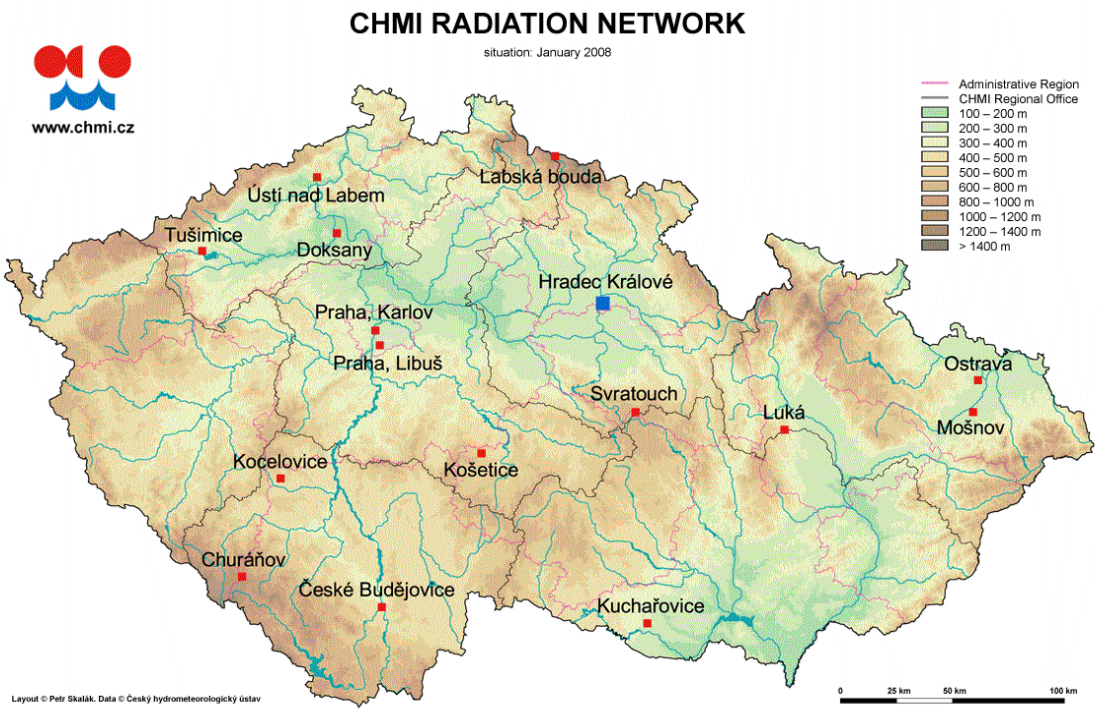

Figure 45 : Map of stations of monitoring global radiation in the network of CHMU

13.1.2. Local and private climatic stations

There are also many climatic stations with the private purpose in Czech Republic. However the network of those stations is not possible to find out. One of this private station provided data measured in Třeboň (South Bohemia). The station is equipped with optical rasters and other solar technologies, and a weather station measuring solar radiation – systems that are all subject to constant monitoring.

I_t	global irradiance	×
N	nb. of the day	×
I_d	diffuse irradiance	×
Φ	relative humidity	×
T_a	air temperature	×
α	solar altitude *	-
p	local air pressure	×

Table 13 : Data provided by Trebon station

*The data for solar altitude were not in the set of data from Trebon. It was necessary to calculate this input data for later calculation with solar models.

13.2. Calculation of solar altitude in Trebon

The equation of solar altitude :

$$sin\alpha = sin\delta sin\phi + cos\delta cos\phi cos\omega$$

$$\alpha = arcsin\alpha(sin\delta sin\phi + cos\delta cos\phi cos\omega)$$

$$\alpha = 90° - \theta_z$$

where

α solar altitude (°)
δ declination of the sun (°)
ϕ latitude (49,004° for Trebon) (°)
ω solar time (azimuth) (°)
θ_z zenith angle of the sun (°)

The time is described by the hour angle ω. The calculation of azimuth (solar time).

$$\omega = 15.H_r - 12$$

where
H_r real solar time (h, °)
$H_r = MET + \frac{4(\lambda z - 15°)}{60°} - \eta$

where
λ_z longitude (14,77 ° for Trebon)
η time deviation due to the elliptic shape of Earth (h)

$\eta = 0{,}125sin(0{,}98°D+29{,}7°M-32°)+0{,}165sin(1{,}96°D+59{,}4°M-38°)$

Declination of the sun

$$\delta = 23{,}45\ sin\ (360\frac{285+n}{365})$$

where

n number of the day (-)

ϕ latitude (°)

The formula for calculation of the average value for the declination:

$\delta = 23{,}45°\sin(29{,}7°M + 0{,}98°D - 109°)\ (°)$ (provides the same result as the first equation)

M number of the month (-)

D number of the day (-)

The declination is equal to the latitude to which the sun ray fall perpendicularly at 12.00h.

The Earth turns of 360°in 24h – in one hour it is 15°.

13.3. Correlation of diffuse radiation – original model

Three models – Erbs, Reinds and Lam and Li were used for calculation of diffuse radiation based on global radiation data measured in Trebon. For the comparison were included values in the interval 50-1100 W.m^{-2}. The correlation between diffuse and global radiation is expressed by the following graphs.

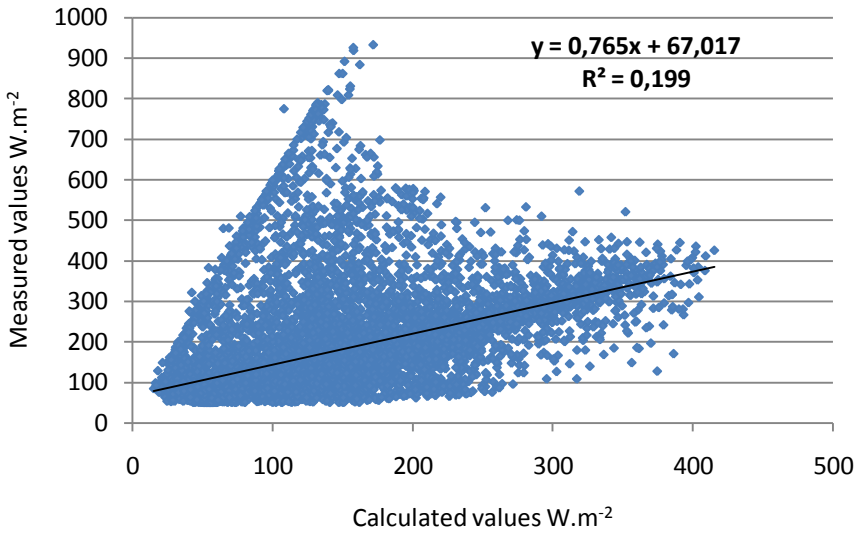

Figure 46 : Graph of correlation of diffuse radiation, original Erbs model for Trebon (2009, 2010)

Figure 46 illustrates the correlation between the values of diffuse radiation measured by pyranomether and the values computationally derived from the Erbs model. In the total of about 11 649 pairs of measured and predicted diffuse radiation values were used to determine the correlation. The correlation coefficient of their linear regression is defined as 0,19.

Computationally derived values of diffuse radiation by Reindl model are compared with measured diffuse irradiance values based on correlation. A total of about 11 526 pairs of measured-predicted diffuse irradiance values were used to determine the correlation coefficient 0,34 .

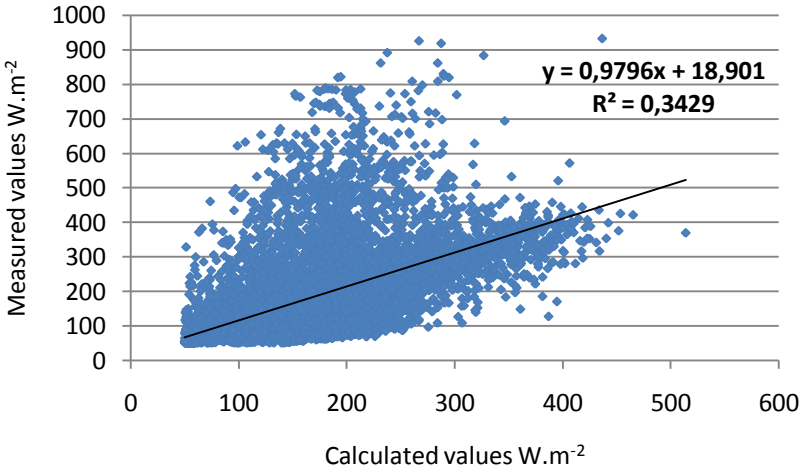

Figure 47 : Graph of correlation of diffuse radiation, original Reindls model for Trebon (2009, 2010)

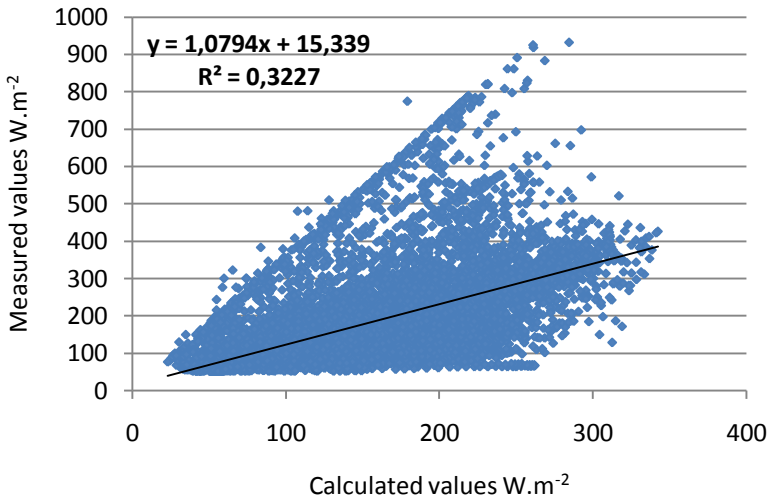

Figure 48 : Graph of correlation of diffuse radiation, original Lam and Li model for Trebon (2009, 2010)

Figure 48 illustrates the correlation between the values of diffuse radiation measured by pyranomether and the values computationally derived from the Lam and Li model. In the total of about 11 649 pairs of measured and predicted diffuse radiation values were used to determine the correlation. The correlation coefficient of their linear regression is defined as 0,32.

Figure 49 illustrates the correlation between the values of diffuse radiation measured by pyranomether and the values computationally derived from the Orgill and Holland´s model. In the total of about 11 649 pairs of measured and predicted diffuse radiation values were used to determine the correlation. The correlation coefficient of their linear regression is defined as 0,219.

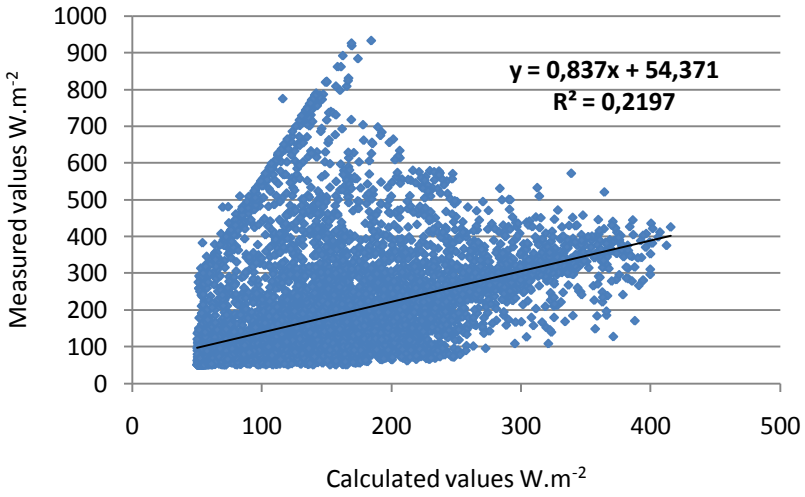

Figure 49 : Graph of correlation of diffuse radiation, original Orgill and Holland model for Trebon (2009, 2010)

13.3.3. Relative error – original model

The relative error between the measurements and predicted derived of diffuse radiation for each model is shown by the Figure 50.

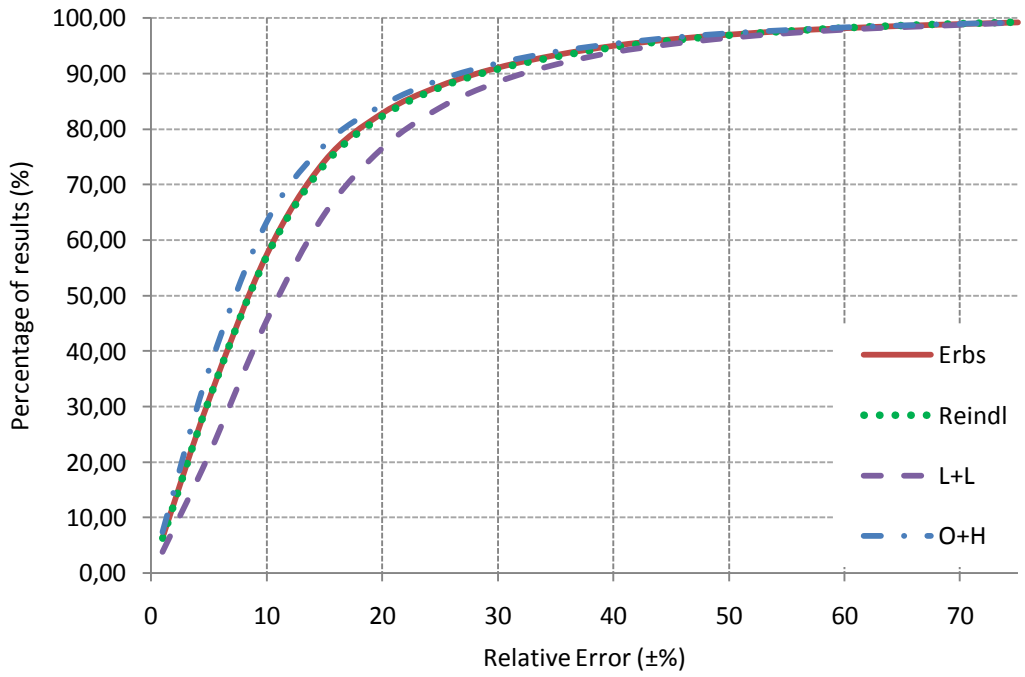

Figure 50 : Relative error of original models (Trebon 2009, 2010)

From graphs of relative error is obvious, that Reindl and Erbs original models provide the higher relative error.

	R^2 orig.	MBD k_d (orig)
Erbs	0,199	15,2
Reindl	0,3429	14,8
Lam and Li	0,3227	16,4
Orgill and Holland	0,2197	14,5

Table 14 : Correlation coefficients for the original model (Trebon 2009, 2010)

	MBD	RMDS
Erbs – orig.	56,88	41,07
Reindl – orig.	52,90	43,24
Lam and Li – orig.	58,70	45,05
Orgill and Holland-orig.	54,96	42,15

Table 15 : Models characteristics for the original model (Trebon 2009, 2010)

13.4. Correlation of diffuse radiation – modified model for Vienna applied on Trebon data

For the comparison of modified models for Vienna was used second data set from Trebon (2009, 2010). There were included values in the interval 50-1100 W.m^{-2}. The correlation between diffuse and global radiation is expressed by the following graphs.

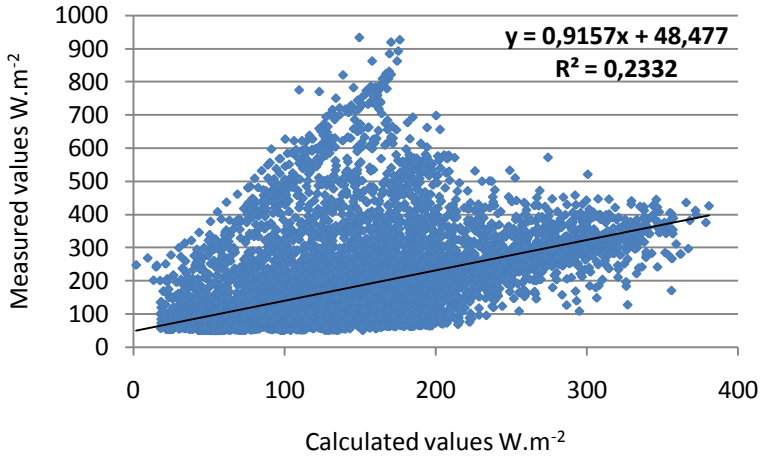

Figure 51 : Graph of correlation of diffuse radiation, Erbs (modif. I) model for Trebon (2009,2010)

Figure 51 shows computationally derived values of diffuse radiation by modified Erbs model are compared with measured diffuse irradiance values based on correlation. A total of about 11 005 pairs of measured-predicted diffuse irradiance values were used to determine the correlation coefficient.

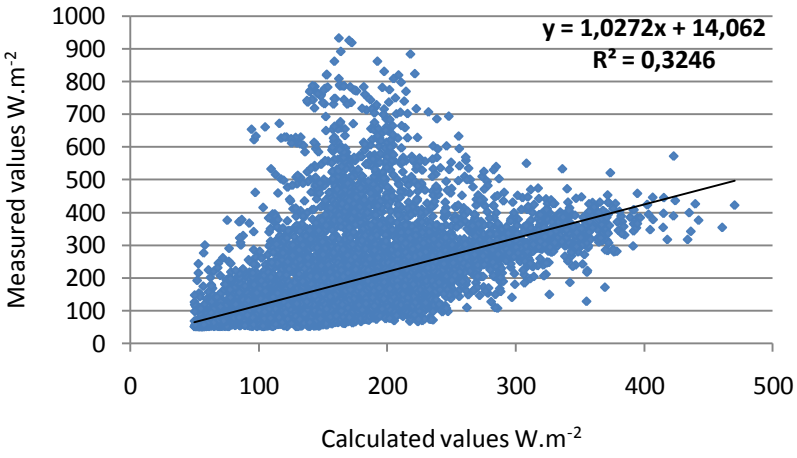

Figure 52 : Graph of correlation of diffuse radiation, Reindl (modif. I) model for Trebon (2009,2010)

Computationally derived values of diffuse radiation by modified Reindl´s model are compared with measured diffuse irradiance values based on correlation. A total of about 10 837 pairs of measured-predicted diffuse irradiance values were used to determine the correlation coefficient 0,32.

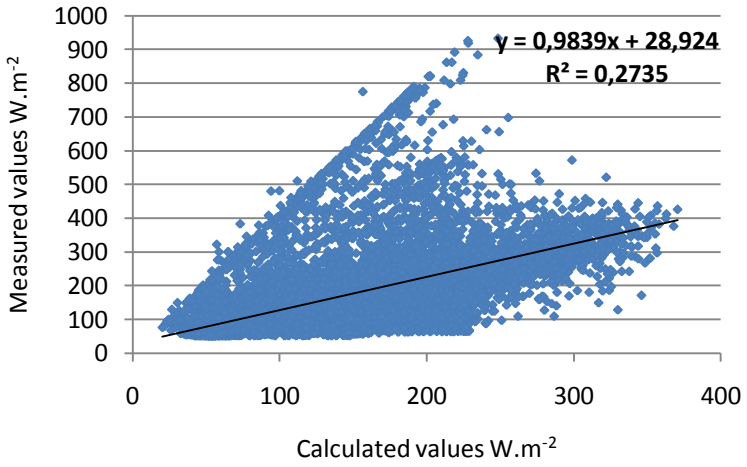

Figure 53 : Graph of correlation of diffuse radiation, Lam and Li (modif. I) model for Trebon (2009,2010)

Figure 53 illustrates the correlation between the values of diffuse radiation measured by pyranomether and the values computationally derived from the modified Lam and Li model. In the total of about 11 005 pairs of measured and predicted diffuse radiation values were used to determine the correlation. The correlation coefficient of their linear regression is defined as 0,27.

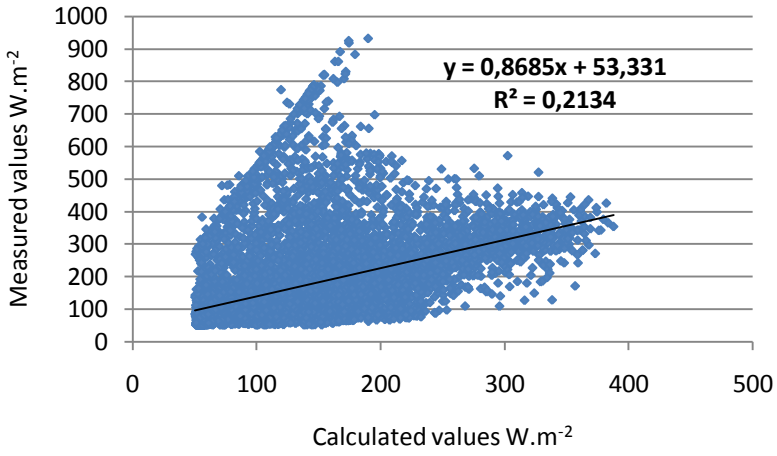

Figure 54 : Graph of correlation of diffuse radiation, Orgill and Holand (modif. I) model for Trebon (2009,2010)

Figure 57 illustrates the correlation between the values of diffuse radiation measured by pyranomether and the values computationally derived from the modified Orgill and Holland model. In the total of about 11 008 pairs of measured and predicted diffuse radiation values were used to determine the correlation. The correlation coefficient of their linear regression is defined as 0,21.

13.4.4. Relative error – modified model

The relative error between the measurements and predicted derived of diffuse radiation for each modified model is shown by the following figure.

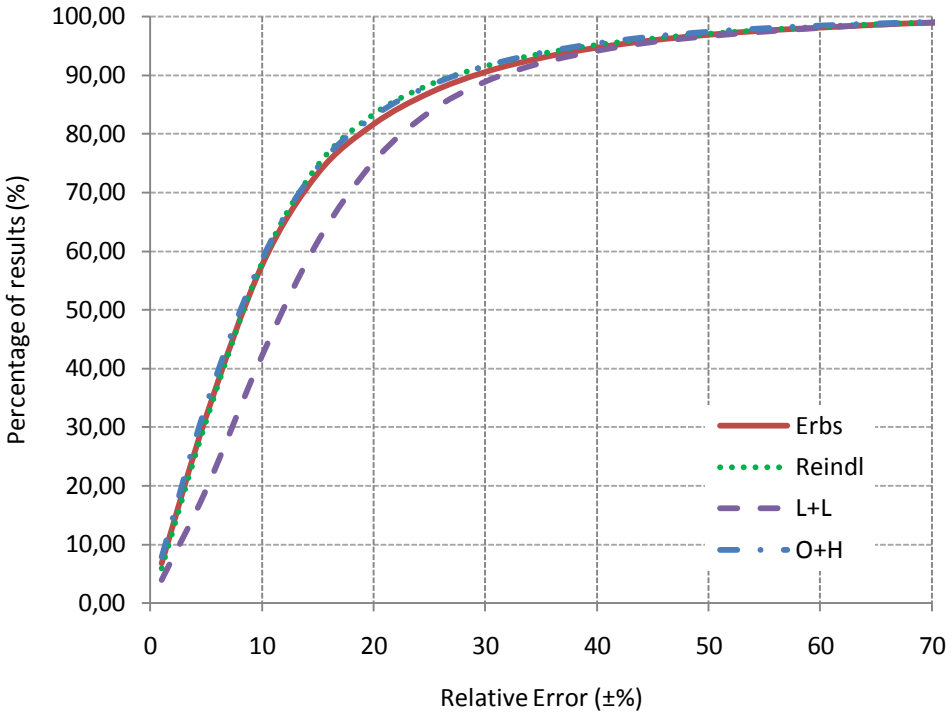

Figure 55 : Relative error of modified (I) models (Trebon 2009, 2010)

From graphs of relative error is obvious, that Lam + Li and Reindls modified models to Vienna provide the higher relative error.

	MDS (modif.I)	**RMDS (modif.I)**
Erbs – modified (I)	57,01	39,35
Reindl – modified (I)	51,37	40,29
Lam and Li - modified(I)	58,11	42,09
Orgill and Holland - modified(I)	56,36	38,70

Table 16 : Models characteristics (modif. I) (Trebon 2009,2010)

14. COMPARISON OF SAME MODELS FOR VIENNA AND TREBON

14.1. Comparison of statistical characteristics

	R^2 orig.	R^2 (modif.I)	MDS kd (orig) %	MDS kd (mod.)%
Erbs - V	0,6934	0,704	10,5	9,2
Reindl - V	0,7436	0,7614	9,9	8,7
Lam and Li - V	0,6281	0,6833	11,9	9,7
Orgill and Holland - V	0,6842	0,6987	11,1	8,9
Erbs - T	0,199	0,2332	15,4	15,5
Reindl - T	0,3429	0,3246	14,8	15,6
Lam and Li - T	0,3227	0,2735	16,5	16,9
Orgill and Holland - T	0,2197	0,2134	14,5	15,3

Table 17 : Correlation coefficients (Trebon – "T", Vienna – "V")

It is obvious, that the modified models for Vienna provide better results in the case of correlation coefficient and average deviation if diffuse fraction compared to the original model for Trebon data.

Compare to the Vienna model calculation are the Trebon models less accurate in correlation coefficient of diffuse radiation. The value of average deviation between measured and calculated diffuse fraction are lower in the case of original model (with original coefficients).

%	MDS orig.	RMDS orig.	MDS modif.I	RMDS modif.I
Erbs - V	32,55	37,43	31,89	33,23
Reindl - V	31,50	37,38	27,55	36,94
Lam and Li - V	41,79	45,67	35,66	39,09
Orgill and Holland - V	35,09	43,09	32,89	34,99
Erbs - T	56,88	41,07	57,01	39,35
Reindl - T	52,90	43,24	51,37	40,29
Lam and Li - T	58,70	45,05	58,11	42,09
Orgill and Holland - T	54,96	42,15	56,36	38,70

Table 18 : Table of characteristics for diffuse radiation (Trebon – "T", Vienna – "V")

It is obvious, that according to the statistical characteristics the modified model for Vienna applied to Trebon data provides better results than the original one for Trebon data, except to the Orgill and Holland model.

14.2. Comparison of relative error

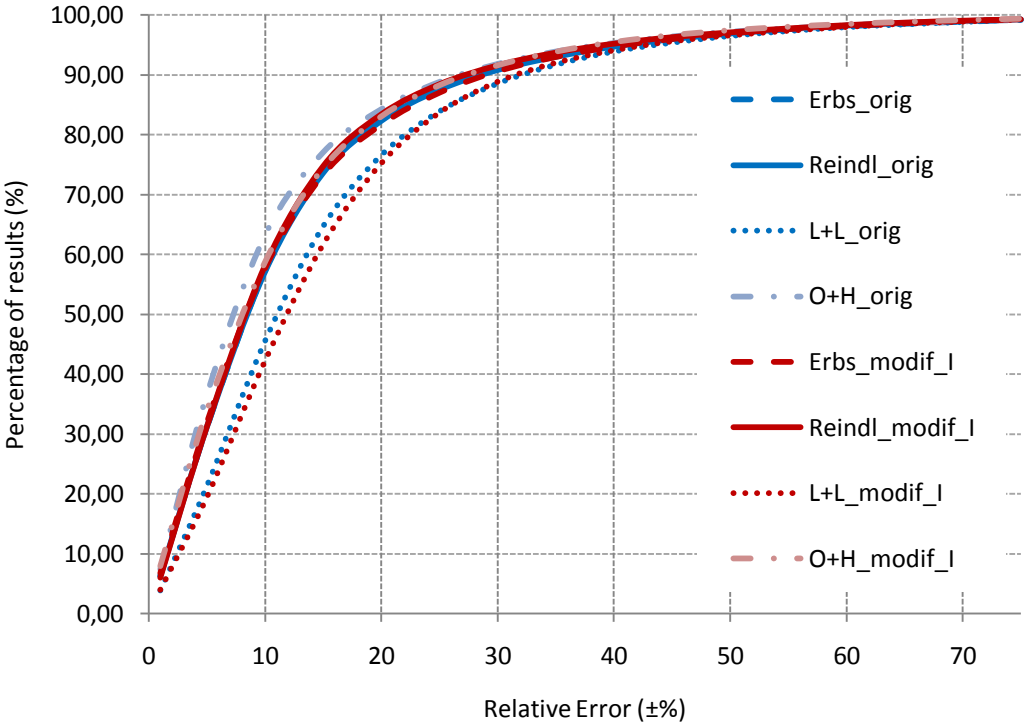

Figure 56 : Relative error of original and modified (I) models (Trebon)

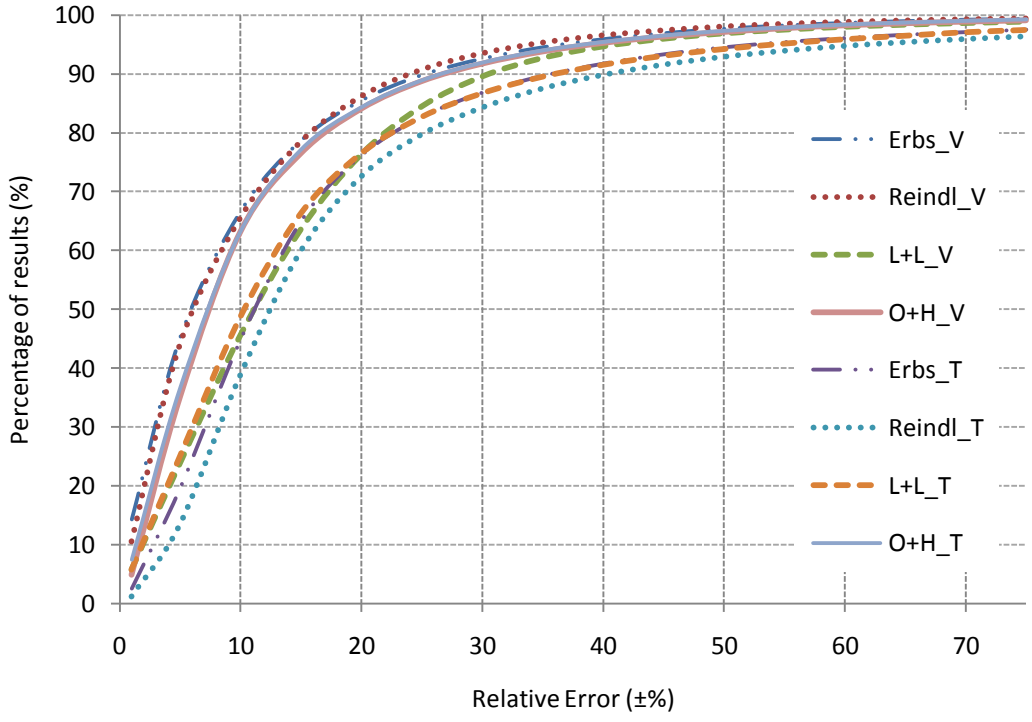

Figure 57 : Relative error of original models (Vienna, Trebon)

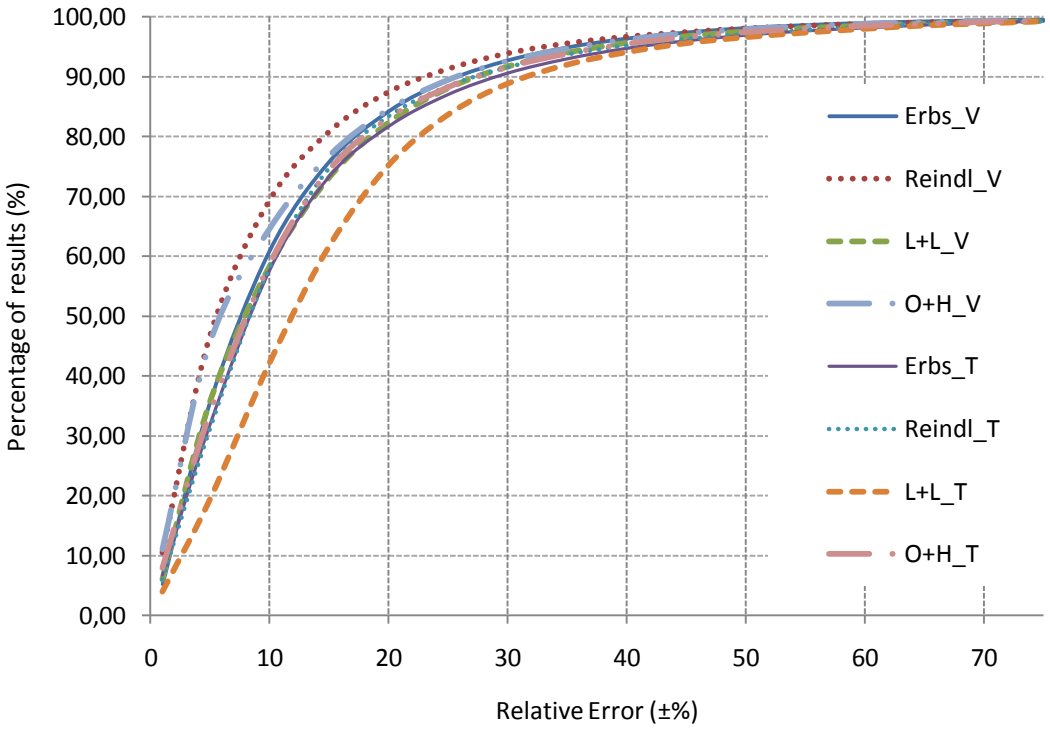

Figure 58 : Relative error of modified models based on Vienna data (Vienna, Trebon)

15. ADAPTATION OF MODELS FOR TREBON DATA

The modification of the coefficients was done throught the software Matlab in the same way as for the data from Vienna.

15.1.1. Modification of Erb´s model

The equation modified for Trebon data:

$$k_d = 1 - 0{,}466k_t \;\; ; \;\; k_t \leq 0{,}22$$

$$k_d = 0{,}1655 + 6{,}629k_t \; - 19{,}3382k_t^2 + 18{,}1028k_t^3 - 5{,}1245k_t^4; \; 0{,}22 < k_t \leq 0{,}8$$

$$k_d = 0{,}2618 \qquad ; \;\; k_t > 0{,}8$$

k_t clearness index (-)
k_d diffuse fraction (-)

15.1.2. Modification of Reindl´s model

The modified equation for Trebon:

Interval : $0 \leq k_t \leq 0{,}3$ Constraint : $I_d/I_t \leq 1{,}0$

$$k_d = 0{,}9965 - 0{,}1452k_t \; + 0{,}0145\sin\alpha - 0{,}006T_a + 0{,}002\Phi$$

Interval : $0{,}3 < k_t < 0{,}78$ Constraint : $0{,}1 \leq I_d/I_t \leq 0{,}97$

$$k_d = 1{,}4263 - 1{,}1899k_t \; - 0{,}0448\sin\alpha - 0{,}0129T_a + 0{,}0035\Phi$$

Interval : $k_t \geq 0{,}78$ Constraint : $I_d/I_t \geq 0{,}1$

$$k_d = 0{,}2448 + 0{,}1608k_t \; - 0{,}2899\sin\alpha + 0{,}0027T_a + 0{,}0102\Phi$$

k_t clearness index (-)
k_d diffuse fraction (-)

15.1.3. Modification of Lam and Li´s model

The modified equation for Trebon:

$$k_d = 0{,}8989; \quad k_t \leq 0{,}15$$

$$k_d = 1{,}2825 - 1{,}3856 k_t; \quad 0{,}15 < k_t \leq 0{,}7$$

$$k_d = 0{,}2188 \quad ; \quad k_t > 0{,}7$$

k_t clearness index (-)
k_d diffuse fraction (-)

15.1.4. Modification of Orgill and Holland´s model

The modified equation for Trebon:

$$k_d = 1 - 0{,}343 k_t; \quad k_t < 0{,}35$$

$$k_d = 1{,}419 - 1{,}367 k_t; \quad 0{,}35v \leq k_t \leq 0{,}75$$

$$k_d = 0{,}254 \quad ; \quad k_t > 0{,}75$$

k_t clearness index (-)
k_d diffuse fraction (-)

15.2. Correlation of diffuse radiation – modified models for Trebon data

Modified models (Erbs, Reindl, Lam and Li. Orgill and Holland) were used for the calculation of diffuse radiation based on first data set (2007, 2008) and the second set for comparison (2009, 2010). For the comparison were included values in the interval 50-1100 W.m^{-2}.

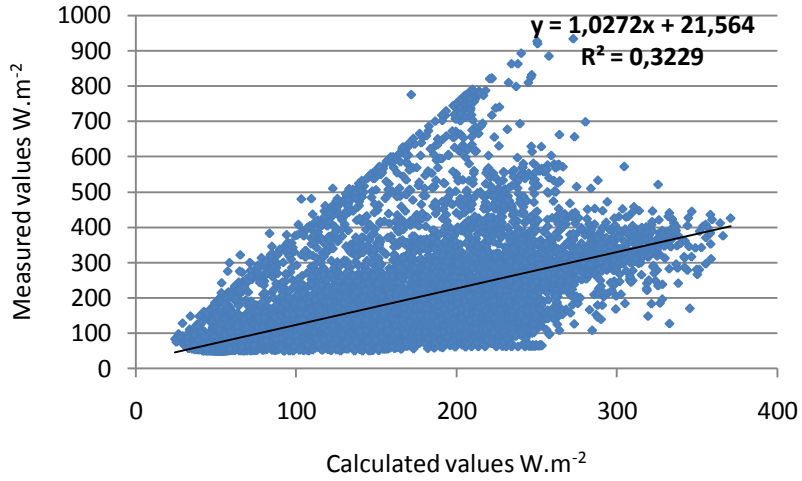

Figure 59 : Graph of correlation of diffuse radiation, Erb´s model for Trebon data modified coefficients (2009,2010)

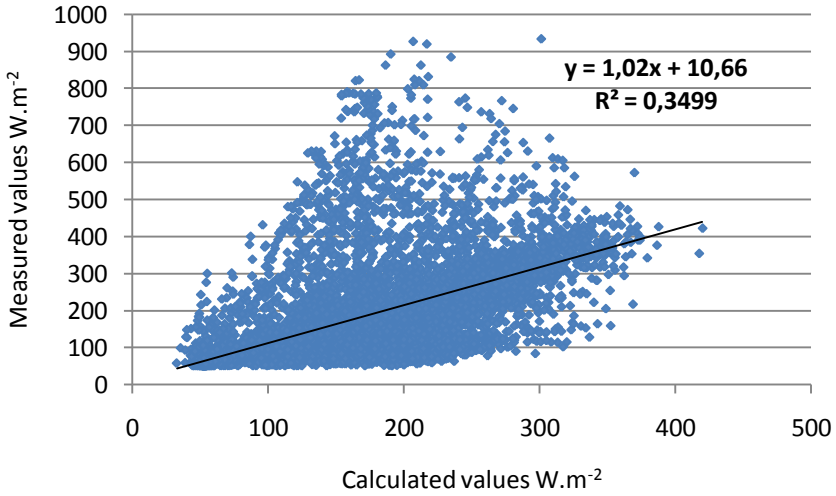

Figure 60 : Graph of correlation of diffuse radiation, Reindl´s model for Trebon data modified coefficients (2009,2010)

Derivation of diffuse irradiance based on measured global irradiance data

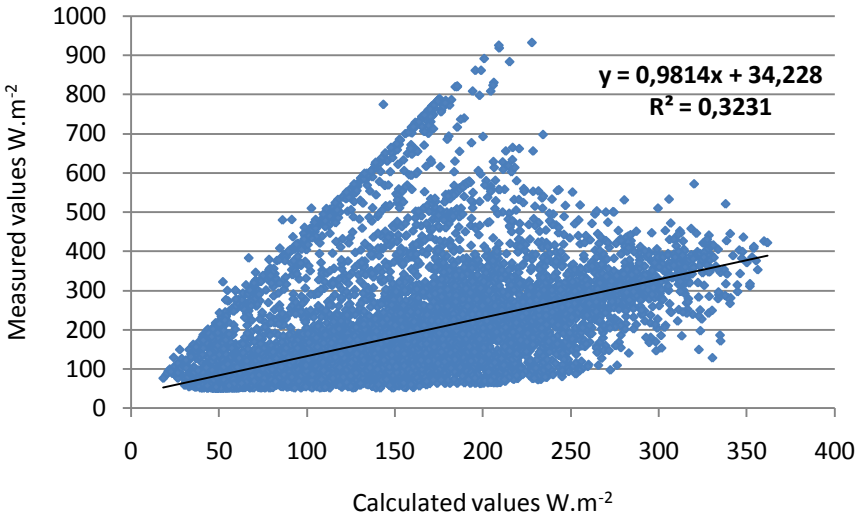

Figure 61 : Graph of correlation of diffuse radiation, Lam and Li model for Trebon data modified coefficients (2009,2010)

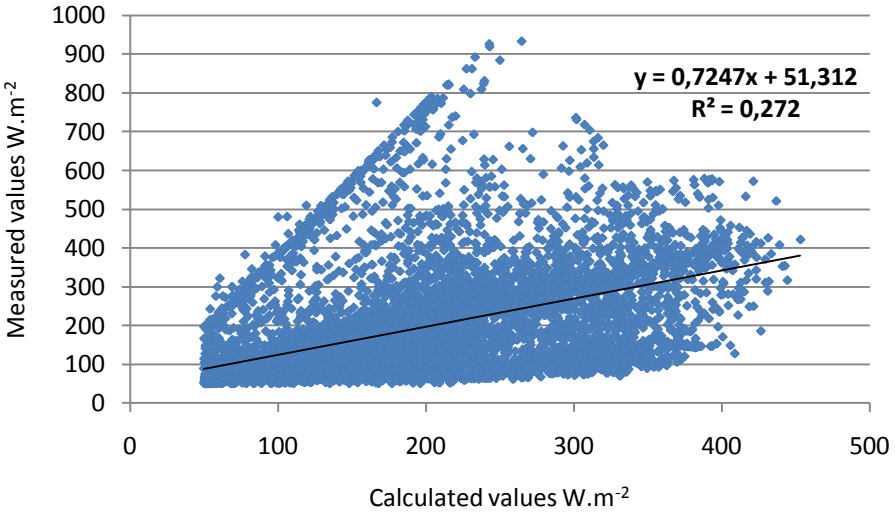

Figure 62 : Graph of correlation of diffuse radiation, Orgill and Holland´s model for Trebon data modified coefficients (2009,2010)

Derivation of diffuse irradiance based on measured global irradiance data

15.2.1. Comparisons of original and modified models (Trebon)

	R^2 orig.	R^2 mod_I	R^2 mod_II	MDS kd (orig) %	MDS kd (mod_I)%	MDS kd (mod_II)%
Erbs	0,199	0,2332	0,3229	15,4	15,5	15,4
Reindl	0,3429	0,3246	0,3499	14,8	15,6	12,4
Lam and Li	0,3227	0,2735	0,3231	16,4	16,9	16,1
Orgill and Holland	0,2197	0,2134	0,272	14,5	15,3	14,4

Table 19 : Correlation coefficients (Trebon – "T")

	MDS (orig)	RMDS (orig)	MDS (mod.I)	RMDS (mod.I)	MDS (mod.II)	RMDS (mod.II)
Erbs	56,88	41,07	57,01	39,35	56,54	39,03
Reindl	52,90	43,24	51,37	40,29	50,31	40,77
Lam and Li	58,70	45,05	58,11	42,09	57,42	42,09
Orgill and Holland	54,96	42,15	56,36	38,70	53,85	54,58

Table 20 : Models characteristics (Trebon 2009,2010)

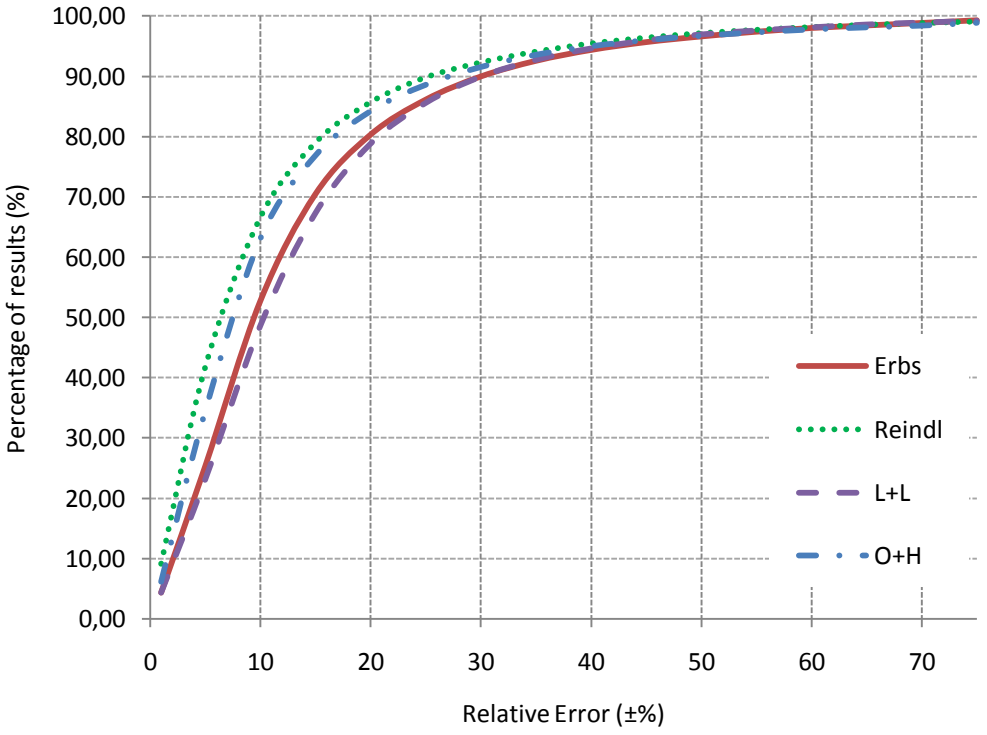

Figure 63 : Relative error of modified models for Trebon, based on Trebon data

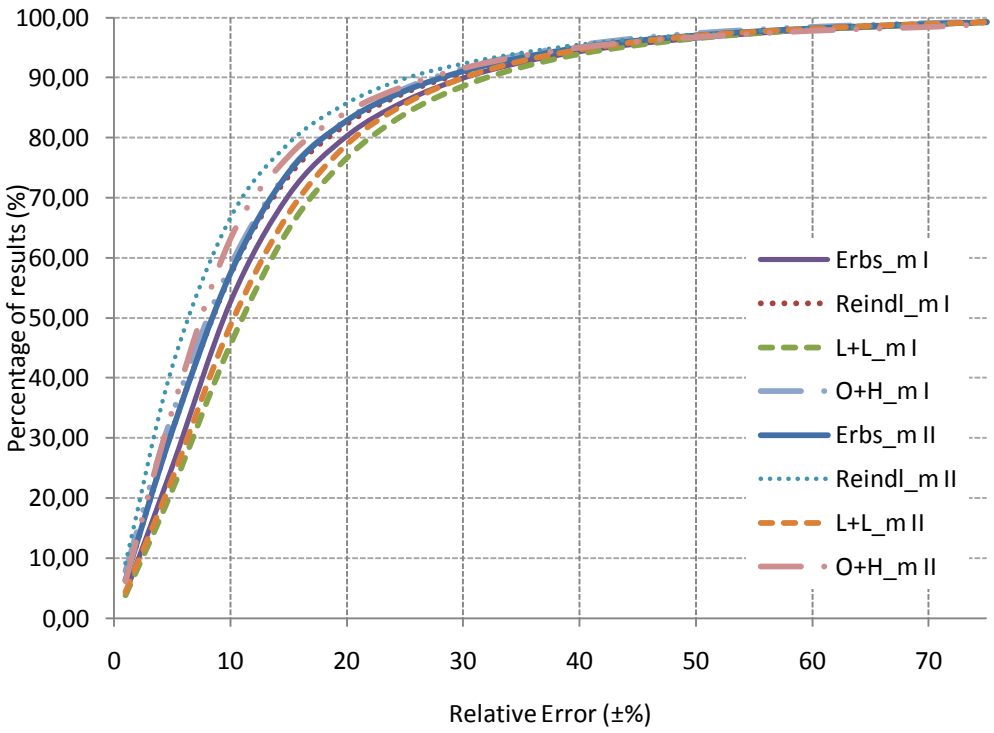

Figure 64 : Relative error of modified models for Trebon, based on Vienna data (I) Trebon data (II)

16. COMPARISON OF MODELS

16.1. Comparison of statistical characteristics

	R^2 orig.	R^2 modif.II	MDS kd (orig) %	MDS kd (modif.II)%
Erbs - V	0,6934	0,704	10,5	9,2
Reindl - V	0,7418	0,7614	9,9	8,7
Lam and Li - V	0,6281	0,6833	11,9	9,7
Orgill and Holland - V	0,6842	0,6987	11,1	8,9
Erbs - T	0,199	0,3229	15,4	15,4
Reindl - T	0,3429	0,3499	14,8	12,4
Lam and Li - T	0,3227	0,3231	16,4	16,1
Orgill and Holland - T	0,2197	0,272	14,5	14,4

Table 21 : Correlation coefficients (Trebon – "T", Vienna – "V")

%	MDS orig.	RMDS orig.	MDS modif.II	RMDS modif.II
Erbs - V	32,55	37,43	31,89	33,23
Reindl - V	31,50	37,38	27,55	36,94
Lam and Li - V	41,79	45,67	35,66	39,09
Orgill and Holland - V	35,09	43,09	32,89	34,99
Erbs - T	56,88	41,07	56,54	39,03
Reindl - T	52,90	43,24	50,31	40,77
Lam and Li - T	58,70	45,05	57,42	42,09
Orgill and Holland - T	54,96	42,15	53,84	54,58

Table 22 : Table of characteristics for diffuse radiation (Trebon – "T", Vienna – "V")

It is obvious, that the modified models provides better results than, the original one for Trebon data.

17. DISCUSSION

The long period of data collection and large amount of data in each set provide quite objective judgement about the performance of four models in derivation of diffuse irradiance. For both location in Austria and Czech Republic were assumed same four models with the use of data for the same years and seasons. The data were cleaned from values measured during the night period, when the solar altitude is lower than 5°. The calculation of diffuse radiation was run with measured values of global irradiation belong to the interval of 50-1100 $W.m^{-2}$. The two different measurements of diffuse irradiance were available for the Vienna set of data. Those data with the higher deviation than 5% between those two measurements were not included. Based on those facts was assumed that the available data represents a good sample of sky conditions and provide good comparison of models.

The first way of comparison was the correlation of measured and calculated diffuse irradiance by eight solar models. The input for both of compared values (measured and calculated diffuse irradiance) was measured data on the same time and place – the calculated diffuse irradiance came from the measured global irradiance. This obtained correct comparison by the correlation. The correlation coefficient as the first evaluation factor describes the accuracy of the calculated values of diffuse calculation. The highest correlation coefficient is provided by the Reindl´s solar model. The Reindl´s original model has also the small range of errors compare to other three models. The deviation between the calculated and measured values of diffuse fraction is the lowest in the case of Reindls original model. Instantly the comparison of original models was completed, the modification of models coefficients could be made. The modification is based on the measured values of diffuse fraction and clearness index.

The improvement of evaluation factors was expected after those mathematical changes of each equation of models. The correlation of diffuse irradiance increases in every case. The best improvement of correlation coefficient appears in the Lam and Li model. The highest range of correlation is given by Reindl´s model. The behaviour of models with modified coefficients is shown by the chart of relative error. It is obvious, that the narrowest of errors is obtained with modified Reindl´s model. The second most

accurate modified model is the Erb´s model. The modified and also the original Orgill and Holland model provide the less error than the original Erbs model. Both of Lam and Li models – original and modified give the highest values of error. The deviation between measured and calculated diffuse fraction is the lowest for the Reindl´s model (both cases). The original Erb´s model has the deviation of measured k_d and calculated k_d lower than the Orgill and Holland´s model. By the modification of coefficients are obtained different deviations and in this case the Orgill and Holland´s model (modif.) provides better values than the Erb´s modified model.

Erb´s model appears to perform better under the clear sky condition. The correlation coefficient for the clear sky is 0,99. MDS as well as RMDS perform the lowest values for this model. Second well behaves model in the condition of clear sky is Lam and Li model. On the other hand Reindls model performs very well in the cloudy sky condition. The correlation coefficient of diffuse irradiance is the highest for Reindl´s model during the cloudy sky. Orgill and Holland´s model gives the low MDS and RMDS in calculation of diffuse irradiance during the cloudy sky. The highest correlation coefficient between measured and calculated diffuse irradiance during the partly cloudy sky condition is provided by the Lam and Li model. The lowest values of MDS and RMDS, during the partly cloudy sky, are provided by the Reindls model.

When the comparison of original and modified models for Vienna was completed, the same process of evaluation was used for the Trebon data set. This evaluation includes three different models. The first model was the original one, the second model for calculation of diffuse radiation was the model with modified coefficients for Vienna set of data and finally the third model has modified coefficients to the Trebon data.

Orgill and Holland´s original model provides the lowest value of relative error for the calculated diffuse radiation in the location of Trebon. The correlation of measured and calculated diffuse radiation perform the highest coefficient in the Reindls original model as well as the lowest MDS. Low value of RMDS is given by the original model of Erbs.

The modified models for Vienna applied to the Trebon data provides, except the Erbs model, the worst results of the diffuse radiation correlation between measured and calculated values than the original models. There is only the improvement of correlation coefficient in the case of Erbs model.

The second modified model that was modified based on Trebon data provides improvements in correlation coefficients, in statistical characteristics and also in relative error. The highest improvement of r^2 is obvious for the Erbs model. The best performed model is Reindls model.

18. CONCLUSION

The estimation of the solar radiation, for instance by solar radiation models, is desirable for designing buildings with a good thermal environment and also solar-energy systems. The purpose of this study was to computationally derive the horizontal diffuse irradiance from measured global irradiance on the horizontal surface. For this thesis four decomposition models were used to predict the diffuse irradiance under a sky of all conditions in Vienna (Austria) and Třeboň (Czech Republic). The comparison of calculated values by those models was made with measured data of diffuse irradiance.

The calculation of diffuse irradiance was performed based on global irradiance values. The computationally derived values of diffuse radiation were compared with the corresponding measurements. Based on the high correlation and low relative error one can deduce that Reindl´s model performs the best of the solar models during a day with changeable sky conditions. The Erb´s model behaves better then Reindl´s model during a day with clear sky conditions.

Modification of the model´s coefficients based on data for each location provides improvements in all cases. However, all modified and original models perform better estimation of diffuse irradiance values for Vienna data than for Trebon data.

For future work on this subject could be advised to use the Reindl´s model to estimate diffuse radiation because this model considers more factors in weather conditions. It can be concluded that the derivation of diffuse irradiance is based on more parameters than only clearness index. The incorporation of other factors provides more accurate results.

19. REFERENCES

[1] L.T. Wong, W.K. Chow, Solar radiation model; Applied Energy 69 (2001) 191-224

[2] Bishop, Ch. Pattern Recognition and Machine Learning., Springer 2006

[3] Department of Architecture, Chongqing University (B), Chongqing, 400045, People's Republic of China; Received 18 October 1999; Solar control for buildings; Tang Mingfang

[4] John L. Wright, Nathan A. KoteySolar absorption by each element in a glazing/shading layer array; ASHRAE Transactions, July, 2006

[5] D.T. Reindl, W.A. Beckman, J.A. Duffie : Diffuse fraction correlations. Solar Energy 1990, 45 (1): 1-7.

[6] Mahdavi A., Dervishi S., A comparison of global luminous efficacy models. Department of Building Physics and Building Ecology

[7] Pavel Hykš, Jozef Hraška. Slnečné žiarenie a budovy. Alfa. Bratislava. 1990

[8] Batlles F.J., Rubio M.A., Tovar J. Empirical modeling of hourly direct irradiance by means of hourly global irradiance. Energy 25 (2000) 675-688

[9] Liu BYH, Jordan R C. The inter-relationship and characteristic distribution of direct, diffuse and total solar radiation. Solar Energy 1960; 4(3); 1-9

[10] Lam JC, Li DHW. Correlation between global solar radiation and its direct and diffuse components. Building and Environment 1996; 31 (6): 527-35.

[11] Louche A., Notton G., Poggi P. Correlations for direct normal and global horizontal irradiations on a French Mediterranean site. Solar Energy 1991; 46 (4):260-6

[12] Mahdavi A., Dervishi S., Approaches to computing irradiance on building surfaces. Department of Building Physics and Building Ecology

[13] Skartveit A., Olseth JA. A model for the diffuse fraction of hourly global radiation. Solar Energy 1987; 38 (4):271-274.

[14] ERbs DG, Klein SA, Duffie JA, Estimation of the diffuse radiation fraction for hourly, daily and monthly – average global radiation. Solar Energy 1982 (4), 293-302

[15] Alam MS, Saha SK, Chowdhury MAK, Rahman M. Simulation of Solar radiation system. American Journal of Applied Sciences 2(4); 751-758, 2005

[16] Posadillo R, Lugue RL. Hourly distributions of the diffuse fraction of global solar irradiation in Cordoba (Spain). Energy Convesions and Management 50 (2009) 223-231.

[17] Posadillo R, Lugue RL. The generation of hourly diffuse irradiation : A model from the analysis of the fluctuation of global irradiance series. Energy Convesions and Management 51 (2010) 627-635.

[18] Muneer T, Munawwar S, Potential for improvement in estimation of solar diffuse irradiance. Energy Convesions and Management 47 (2006) 68-86.

[19] Detlev Heinemann. Energy Meteorology. Carl von Ossietzky Universitat. Oldenburg 2000.

[20] Fayadh M. Abed Al-Dulaimy, Ph.D. and Ghazi-Yousif-Mohammed Al-Shahery, D.Sc. Estimation of Global Solar Radiation on Horizontal Surfaces over Haditha, Samara, and Beji, Iraq. The Pacific Journal of Science and Technology. Vol. 11.2010

[21] Barakat SA. Comparison of models for calculating solar radiation on tilted surfaces. Proceedings of the Fourth International Symposium on the Use of Computers for Environmental Engineering Related to Buildings. Tokyo, Japan, 1983

[22] BAnnert P, Švejnar Lubor. Fotovoltaický geografický informační system – PVGIS. Vyšší odborná škola a Střední průmyslová škola Varnsdorf. 2009

[23] http://users.zoominternet.net/~matto/Java/Solar%20Calculator.htm

[24] http://www.satellight.com/guide/glosatod.htm

[25] http://www.sciencedirect.com/

APPENDIX

Correlation of diffuse radiation according to the seasons

Data set (data 2008,2009, 2010) was divided in four groups according to the season – winter (December, January, February); spring (March, April, May); autumn (September, October, November); summer (June, July, August). Each season set was used to create correlation between measured and predicted diffuse radiation.

Erb´s model

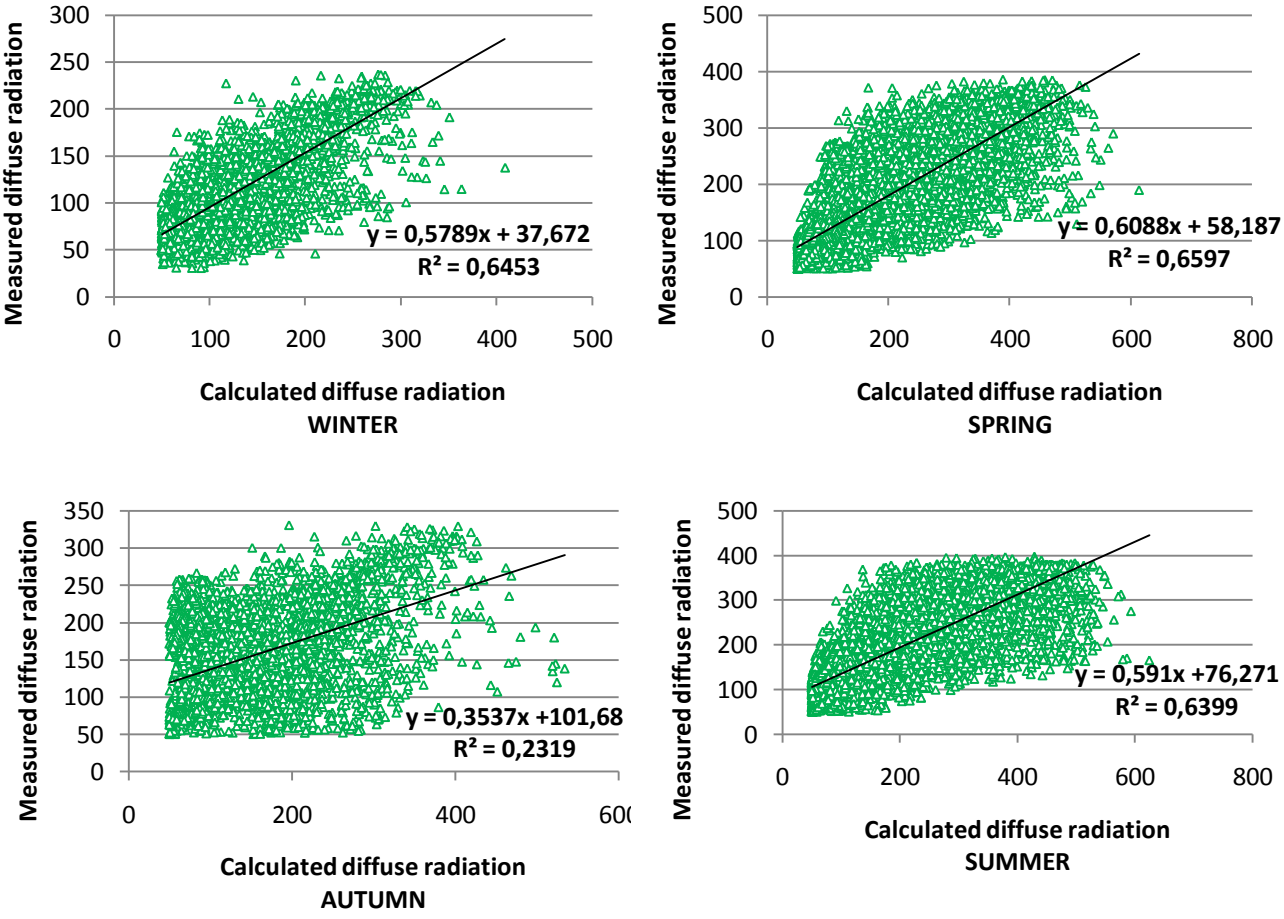

Figure 65: : Correlation between the values measured (I_d) and derived by **modified** Erbs model – seasons

It can be seen from charts above, that according to the correlation of I_d, the best result is provided by the Erbs model for the spring season. The value of r^2 is 0,66. The worst results are given for the autumn season. The value of r^2 is 0,23 for autumn.

Reindl´s model

The charts below show the relation of correlation between measured and calculated I_d according to the seasons. Reindls model provides the same conclusion as the Erbs model. The calculations are more proper for the spring season. The value of r^2 is 0,72 for spring.

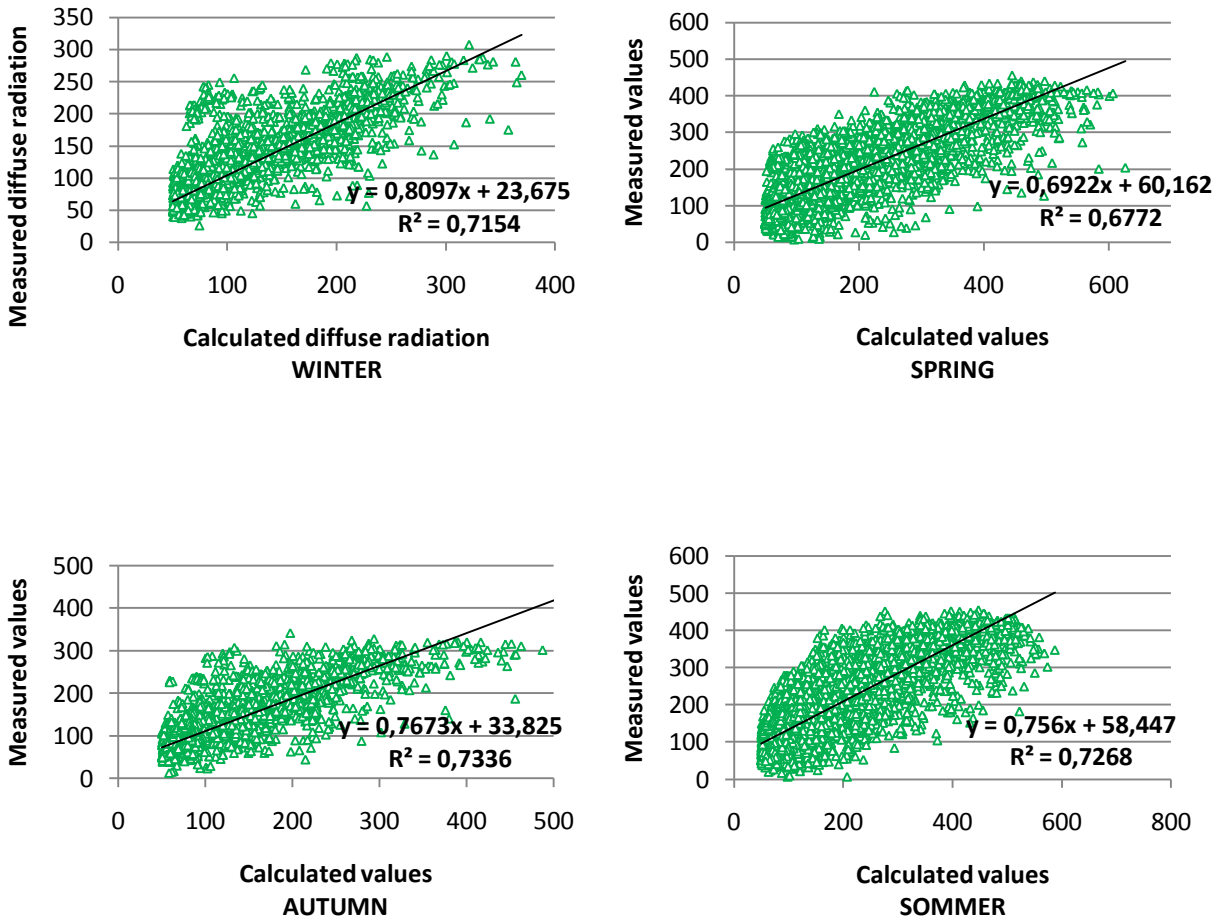

Figure 66: : Correlation between the values measured (I_d) and derived by modified Reindls model – seasons

The lowest value of r^2 is provided for the autumn season like in the case of Erbs model. The value of r^2 is 0,27 for autumn.

Lam and Li model

From the charts below is obvious the difference of results compare to the Erbs and Reindls models. Lam and Li provides the best result of correlation for the winter season.. The value of r^2 is 0,71 for the winter. In the contrast to the Erbs and Reindl model the low accuracy is given for the spring season

.

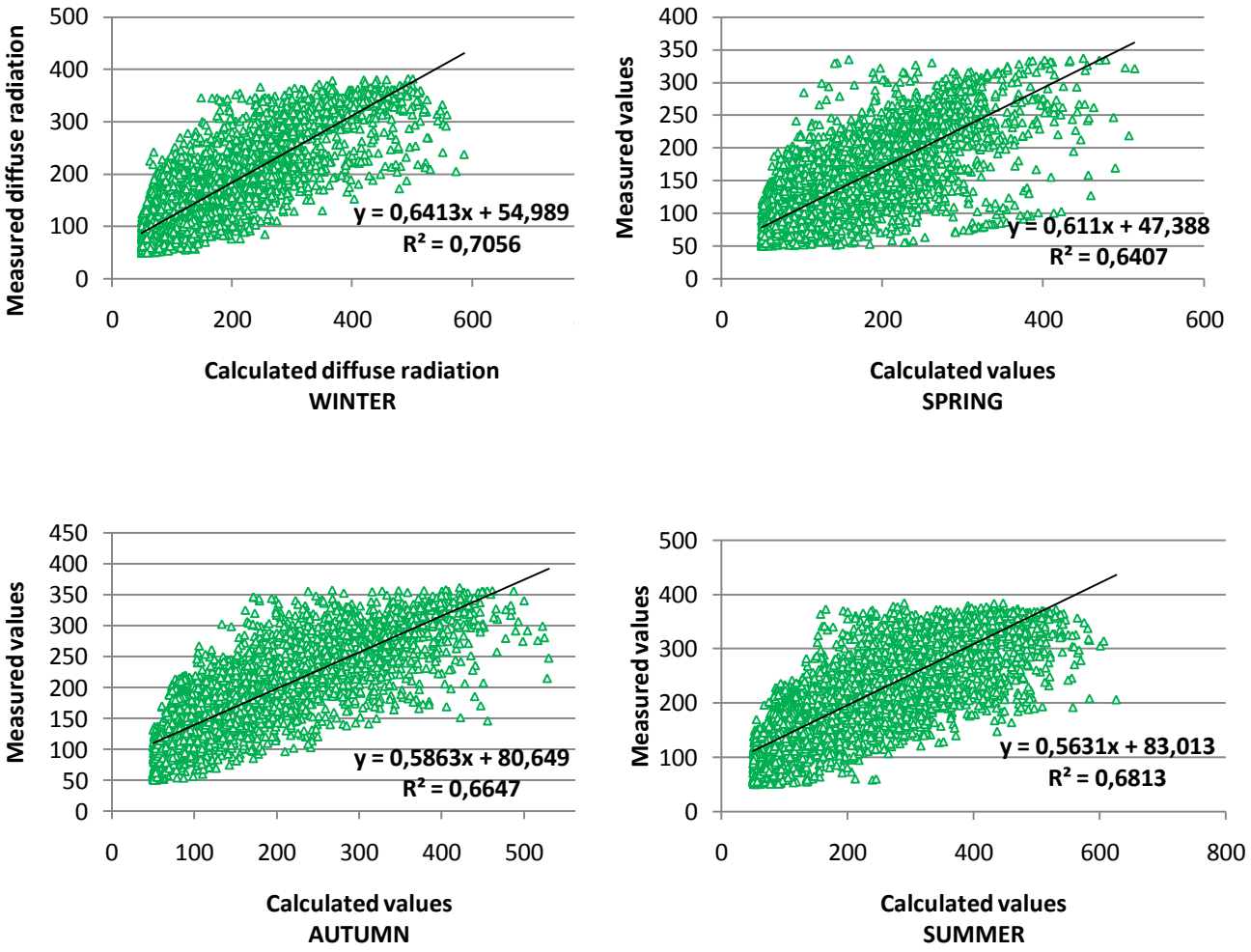

Figure 67: : Correlation between the values measured (Id) and derived by modified Lam and Li model – seasons

Relative error according to the seasons

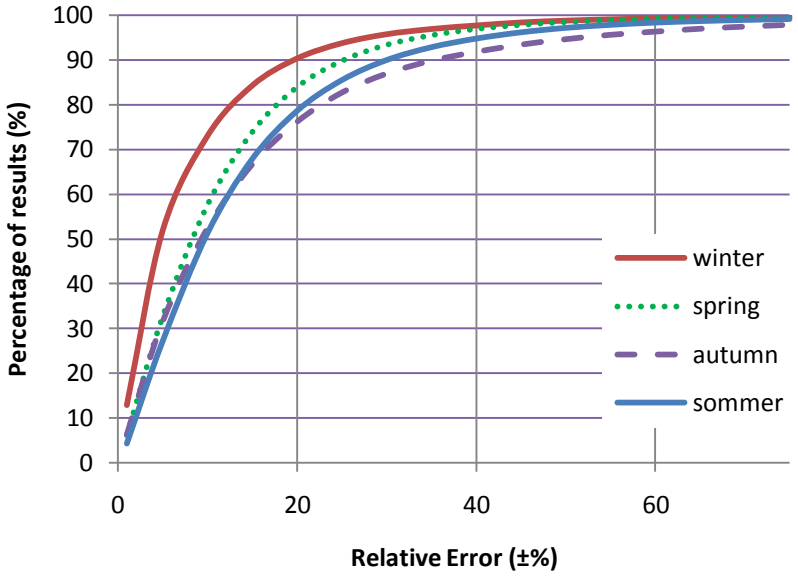

Figure 68 : Percentage of the results with maximum Relative Error for Erbs model with modified coefficients, different seasons

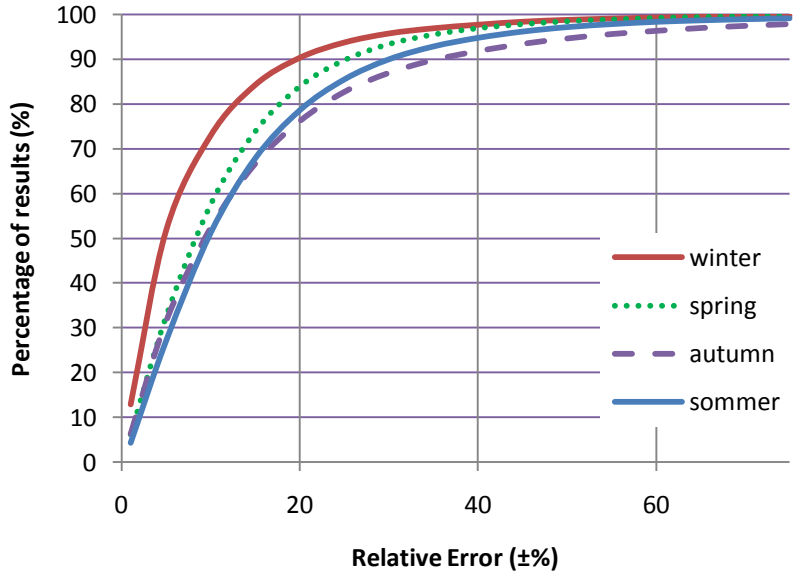

Figure 69 : Percentage of the results with maximum Relative Error for Reindls model with modified coefficients, different seasons

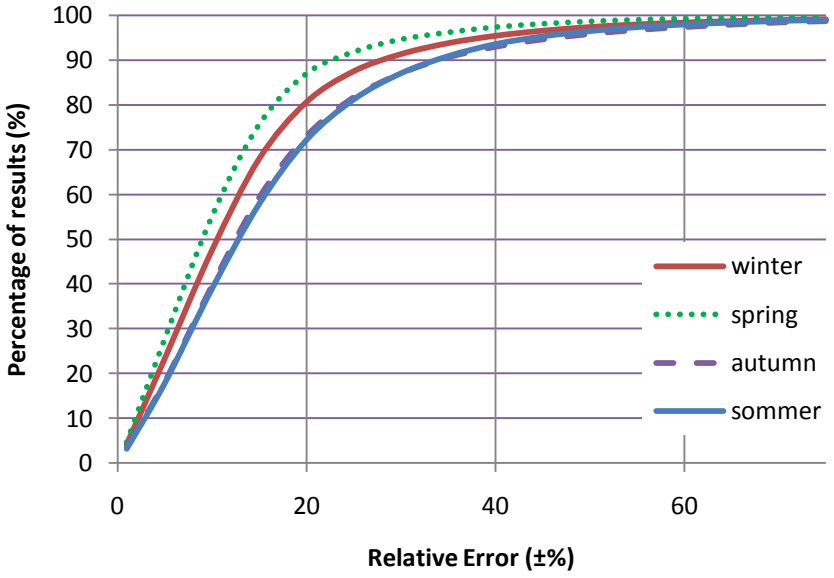

Figure 70 : Percentage of the results with maximum Relative Error for Lam and Li model with modified coefficients, different seasons

From graphs of relative error is obvious, that Erbs and Reindls models provide the higher relative error for winter season and in the contrast the model by Lam and Li gives the highest relative error for the spring season.

RE	1	5	10	15	20	25	30	35	40	45	50	55	60	65	70	75
Erbs	5,16	35,70	60,96	75,81	84,25	89,44	92,76	94,93	96,42	97,43	98,18	98,67	99,03	99,28	99,47	99,60
Reindl	6,93	40,93	64,37	77,93	85,89	90,54	93,37	95,23	96,48	97,35	98,01	98,46	98,80	99,04	99,24	99,38
Lam and Li	10,58	29,84	48,84	65,34	77,27	84,99	89,89	92,90	94,81	96,08	96,96	97,59	98,06	98,41	98,69	98,93
Orgill and Holland	4,89	35	63,1	76,5	84,1	88,7	91,7	93,8	95,2	96,3	97,1	97,8	98,2	98,6	98,9	99,1

Figure 71 : Relative Error – Vienna – original model

RE	1	5	10	15	20	25	30	35	40	45	50	55	60	65	70	75
Erbs	14,21	45,12	66,60	78,67	85,50	89,82	92,60	94,54	95,91	96,94	97,69	98,25	98,68	99,00	99,23	99,40
Reindl	10,45	46,72	69,34	80,81	87,46	91,32	93,92	95,59	96,71	97,48	98,09	98,53	98,85	99,10	99,27	99,40
Lam and Li	5,95	35,69	58,26	73,09	82,31	88,05	91,67	93,99	95,64	96,74	97,53	98,11	98,51	98,82	99,08	99,25
Orgill and Holland	11,00	45,56	64,59	76,78	84,55	89,48	92,63	94,68	96,19	97,24	97,96	98,47	98,86	99,15	99,35	99,50

Figure 72 : Relative Error – Vienna – modified model

RE	1	5	10	15	20	25	30	35	40	45	50	55	60	65	70	75
Erbs	4,34	25,30	52,71	70,44	80,29	86,10	89,94	92,53	94,34	95,64	96,58	97,36	97,98	98,40	98,82	99,27
Reindl	6,27	31,17	57,07	73,59	82,29	87,47	90,78	92,99	94,69	95,92	96,87	97,61	98,20	98,63	98,96	99,24
Lam and Li	3,83	21,26	45,48	64,68	76,57	83,89	88,54	91,68	93,89	95,37	96,49	97,32	97,97	98,43	98,83	99,28
Orgill and Holland	6,12	34,4	63,1	76,9	84,2	88,6	91,5	93,6	95,0	96,0	96,7	97,3	97,8	98,1	98,4	98,9

Figure 73 : Relative Error – Trebon – original model

RE	1	5	10	15	20	25	30	35	40	45	50	55	60	65	70	75
Erbs	6,80	31,92	57,67	73,33	81,71	87,05	90,61	93,01	94,76	96,01	96,96	97,67	98,18	98,65	99,04	99,30
Reindl	5,96	31,16	58,11	74,73	83,40	88,43	91,59	93,72	95,22	96,31	97,11	97,77	98,32	98,74	99,07	99,29
Lam and Li	3,98	19,44	42,21	61,68	75,25	83,70	88,88	92,04	94,13	95,63	96,63	97,40	98,03	98,59	98,93	99,31
Orgill and Holland	7,89	33,84	58,66	74,39	83,01	88,22	91,55	93,84	95,45	96,60	97,41	98,01	98,47	98,82	99,12	99,35

Figure 74 : Relative Error – Trebon – modified (I) model

RE	1	5	10	15	20	25	30	35	40	45	50	55	60	65	70	75
Erbs	6,33	31,09	57,30	74,16	82,81	87,77	91,05	93,31	94,99	96,16	97,01	97,68	98,18	98,59	98,92	99,22
Reindl	9,15	41,78	66,63	79,04	85,75	89,87	92,35	94,14	95,50	96,47	97,21	97,77	98,22	98,60	98,89	99,14
Lam and Li	4,33	23,11	48,63	67,31	78,83	85,59	89,94	92,74	94,63	95,96	96,96	97,62	98,13	98,60	98,94	99,21
Orgill and Holland	7,42	36,57	63,22	77,09	84,31	88,87	91,87	93,95	95,37	96,46	97,27	97,84	98,33	98,68	98,97	99,22

Figure 75 : Relative Error – Trebon – modified (II) model